

# Robust Pricing of Equity-Indexed Annuities under Uncertain Volatility and Stochastic Interest Rate

LUDOVIC GOUDENEGE\*

ANDREA MOLENT†

ANTONINO ZANETTE‡

---

## Abstract

In this paper, we propose a novel methodology for pricing equity-indexed annuities featuring cliquet-style payoff structures and early surrender risk, using advanced financial modeling techniques. Specifically, the market is modeled by an equity index that follows an uncertain volatility framework, while the dynamics of the interest rate are captured by the Hull-White model. Due to the inherent complexity of the market dynamics under consideration, we develop a numerical algorithm that employs a tree-based framework to discretize both the interest rate and the underlying equity index, enhanced with local volatility optimization. The proposed algorithm is compared with a machine learning-based algorithm. Extensive numerical experiments demonstrate its high effectiveness. Furthermore, the numerical framework is employed to analyze key features of the insurance contract, including the delineation of the optimal exercise region when early surrender risk is incorporated.

*Keywords:* Equity-indexed Annuities; Uncertain Volatility Model; Stochastic interest Rate; Tree Method; Machine Learning.

---



---

\*Laboratoire de Mathématiques et Modélisation d'Évry (LaMME), CNRS UMR 8071, Université Paris-Saclay Évry, France  
- ludovic.goudenege@math.cnrs.fr

†Dipartimento di Scienze Economiche e Statistiche, Università degli Studi di Udine, Italy - andrea.molent@uniud.it

‡Dipartimento di Scienze Economiche e Statistiche, Università degli Studi di Udine, Italy - antonino.zanette@uniud.it

# 1 Introduction

Equity-linked annuities (ELAs) are significant contracts in the insurance market, offering interest credits and benefit payouts linked to the performance of one or more equity indices, such as the S&P 500. Among these, equity-indexed annuities (EIAs) stand out for their unique combination of features: they guarantee a minimum rate of return while also allowing policyholders to benefit from additional earnings tied to the performance of the associated indices. These instruments provide a compelling blend of market-linked growth potential and downside protection. The guaranteed minimum interest rate ensures that policyholders retain a baseline value for their investment, even in unfavorable market conditions. This combination of security and growth potential has driven the popularity of EIAs, particularly among individuals focused on retirement planning, who seek a prudent balance between risk and reward. The payoffs of the most common EIA contracts follow a cliquet-style structure, meaning they are determined through a series of periodic resets, with gains secured at each reset point. Such a feature is also known as ratchet, symbolizing the mechanism by which the accrued value can only move upward or remain fixed, never decreasing.

In the early studies on this topic, EIAs were priced under the assumption that the underlying equity index follows a geometric Brownian motion with a constant interest rate, in line with standard financial modeling approaches, as discussed by Gerber and Shiu [8] and Hardy [12]. However, given the typically long maturities of EIAs, it is more appropriate to price these contracts under a stochastic interest rate model rather than relying on a constant rate. The Vasicek model has been one of the first stochastic interest rate framework applied to EIA pricing. Specifically, Sheldon and Tan [23] use Monte Carlo simulations to derive prices for various types of EIAs within the Vasicek framework. Building on this, Kijima and Wong [19] develop a closed-form pricing formula for ratchet EIAs with geometric index averaging under the extended Vasicek model. They also introduce an efficient Monte Carlo simulation algorithm for pricing EIAs with arithmetic index averaging. Furthermore, as highlighted by Kijima and Wong [19], the EIA pricing literature has largely overlooked early surrender risk. Moreover, they identified addressing this oversight as a compelling and open problem in the field. To this aim, Wei et al. [27] focus on improving the pricing of EIAs, particularly those with ratchet features, minimum contract values and early surrender options.

Later, some authors have focused on describing the dynamics of the underlying by considering stochastic volatility models and jump-diffusion models. In this regard, Windcliff et al. [11] examine several numerical methods and volatility models for valuing cliquet options, and they focus on the impacts of different volatility assumptions, such as local volatility surfaces, jump-diffusion models, and uncertain volatility models. More recently, Hieber [15] introduces a regime-switching Lévy model to value equity-linked life insurance contracts with annual cliquet-style return guarantees and incorporates macroeconomic regime changes via a Markov chain. Cui et al. [6] develop an efficient method for pricing ELAs with cliquet-style guarantees using advanced models such as regime-switching Lévy processes and stochastic volatility models with jumps. Hess [14] addresses the pricing of cliquet options within a jump-diffusion Lévy framework. In this model, the underlying stock price process incorporates both Brownian motion and compound Poisson jumps, capturing rare market events such as crashes or sudden upward movements.

It is widely recognized that cliquet options exhibit significant sensitivity to unpredictable future changes in the volatility skew, as discussed by Windcliff et al. [11], among others. Relying on constant or local volatility models, such as Dupire's framework, can result in substantial mispricing, necessitating more sophisticated approaches to volatility modeling. Stochastic volatility models like Heston or Hull-White, as well as hybrid jump-diffusion models, typically involve a challenging and sometimes unreliable calibration process. Furthermore, the effectiveness of delta hedging strategies within these models is often unclear, as noted by Hess [14]. Unlike many other exotic derivatives, the valuation of a cliquet option is particularly dependent

on the choice of model used to calibrate against vanilla option prices and a careful modeling for volatility is particularly important for these products because of the non convex nature of their payoff function. Given these complexities, several experts in applied mathematical finance, such as Wilmott [28], Windcliff et al. [11], Hénaff and Martini [13], have advocated for the use of the Uncertain Volatility Model (UVM), which provides a robust framework for both pricing and evaluating the volatility risk associated with structured products containing embedded cliquet options. Specifically, the UVM, introduced by Avellaneda et al. [1], bounds the volatility of the underlying within predefined limits. Such a model ensures robust pricing even under significant market uncertainty, making it highly applicable for exotic options and derivatives that are sensitive to volatility fluctuations.

Recently, researchers have increasingly explored the integration of the UVM with stochastic interest rate frameworks in the valuation of financial derivative instruments. The combination of these two models allows for a robust management of market uncertainties by addressing the dual complexities of random volatility and the fluctuating dynamics of interest rates. This synergy is particularly effective when traditional stochastic processes struggle to fully capture the variability in market conditions. The UVM, by keeping volatility within specified bounds, enables robust pricing strategies even in the presence of considerable market uncertainty. This makes it particularly effective for exotic options and derivatives with high sensitivity to volatility dynamics. Meanwhile, stochastic interest rate models, such as those based on Hull-White or CIR (Cox-Ingersoll-Ross) processes, provide a realistic representation of interest rate movements, which are crucial for accurate pricing in fixed-income markets or derivatives tied to rate-sensitive assets. For instance, the integration of these models has been particularly useful in pricing cliquet options and equity-linked products, where path dependency and market conditions introduce additional layers of complexity. In this regard, Hölzermann [16, 17] examines the classical Hull-White model for interest rate term structures while incorporating volatility uncertainty, and proposes a new approach to pricing zero-coupon bonds and interest rate derivatives. Recently, Wang [26] addresses the problem of pricing European call options under uncertainty in both volatility and the risk-free interest rate, and he proposes a numerical method based on a partial derivative equation and an interior penalty method to solve the discretized optimization problem which arises in this context. This integrated approach continues to gain traction as it bridges the gap between theoretical modeling and practical market application, offering enhanced tools for risk management and pricing under uncertainty. All of these advancements have significant implications for financial engineering, especially in stress-testing and hedging strategies for derivative portfolios.

This paper explores the combined effect of an uncertain volatility model and a stochastic interest rate on EIAs. Specifically, the proposed stochastic model extends the UVM by allowing the interest rate to follow a stochastic process. Under risk-neutral probability, we consider a model in which the risk-free rate is described by the Hull-White model, while the underlying equity index of the EIA contract evolves according to a geometric Brownian motion with a growth rate equal to the risk-free rate and an unknown but bounded volatility. This modeling development enables a deeper analysis of EIAs and reveals relationships that, to the best of our knowledge, have not been previously reported in the literature. Moreover, the proposed robust stochastic model contributes to the existing literature by examining the pricing of these products when policyholders have the option to terminate the contract before its stipulated maturity date. In particular, following Wei et al. [27], we study these contracts with early surrender option under uncertain volatility and stochastic interest rate. The model is of particular interest because, as Smith observed in [24], there are different ways of defining the concept of option price, since the writer and the buyer, who are trying to hedge against speculative risks, have different optimal exercise strategies. These remarkable results are made possible by the development of an efficient numerical pricing method specifically designed for this model. The proposed pricing algorithm, termed Tree UVHW, interprets the pricing of a derivative instrument as a local

optimization problem that can be solved by resorting to a tree structure and extending it to the stochastic interest rate. In particular, Tree UVHW uses a tree structure to spread the interest rate in addition to a tree approach for the underlying. An optimization algorithm for optimal volatility computation and interpolation to handle different possible values of the underlying volatility are also included. The proposed algorithm is tested against an adapted version of the GTU algorithm introduced by Goudenège et al. [10], which, in contrast, leverages machine learning techniques. Whenever feasible, results from the Monte Carlo method are also used as a benchmark for comparison. The results obtained highlight the high accuracy of the Tree UVHW method and the reduced computational time.

The remainder of the paper is structured as follows. Section 2 introduces the financial model that underpins our investigation. Section 3 presents our novel tree-based numerical algorithm for option pricing within the proposed stochastic framework. Section 4 details the structure of the EIA contract, highlighting its cliquet-style payoff features and the incorporation of early surrender risk. Section 5 discusses the application of the proposed Tree UVHW algorithm to EIA pricing. Section 6 explains how the GTU algorithm can be adapted for EIA valuation. Finally, Section 7 provides an extensive set of numerical experiments to validate our methodology and explore the characteristics of these insurance contracts.

## 2 The financial market model

Let  $S = (S_t)_{t \in [0, T]}$  denote the value of the underlying equity index, which evolves according to the uncertain volatility model. Specifically, under a suitable risk-neutral probability measure  $\mathbb{Q}$ , the dynamics of  $S$  are governed by the stochastic differential equation

$$dS_t = (r_t - \eta) S_t dt + \sigma(t, S_t, r_t) S_t dW_t^S, \quad (2.1)$$

where  $S_0 = s_0 > 0$  is the initial spot price,  $r_t$  is the stochastic short rate,  $\eta$  is the constant dividend yield,  $\sigma(t, S_t, r_t)$  is the time- and state-dependent volatility, and  $W^S = (W_t^S)_{t \in [0, T]}$  is a standard Wiener process. In the UVM, the volatility  $\sigma(t, S_t, r_t)$  varies within known bounds:

$$\sigma_{\min} \leq \sigma(t, S_t, r_t) \leq \sigma_{\max}, \quad (2.2)$$

where  $\sigma_{\min}$  and  $\sigma_{\max}$  are positive constants. For the sake of brevity, we will write  $\sigma$  instead of  $\sigma(t, S_t, r_t)$ , thus omitting the dependency of volatility on time, the underlying value, and the interest rate.

Here, we assume that the short rate  $r = (r_t)_{t \in [0, T]}$  evolves according to the Hull-White model under  $\mathbb{Q}$ :

$$dr_t = \kappa(\theta(t) - r_t) dt + \omega dW_t^r, \quad (2.3)$$

where  $\kappa > 0$  is the mean-reversion rate,  $\theta(t)$  is a deterministic function ensuring the model fits the term structure,  $\omega > 0$  is the volatility of the short rate, and  $W^r = (W_t^r)_{t \in [0, T]}$  is a standard Wiener process such that  $d\langle W_t^S, W_t^r \rangle = \rho dt$ . As is common practice (see e.g. Brigo and Mercurio [3]), we define the market instantaneous forward rate at time  $t = 0$  for a maturity  $T$  as

$$f^M(0, T) = -\frac{\partial \ln P^M(0, T)}{\partial T}, \quad (2.4)$$

where  $P^M(0, T)$  denotes the market price of a zero-coupon bond at  $t = 0$  with maturity  $T$ . The following equation facilitates the unique definition of the function  $\theta_t$ , thereby ensuring that theoretical zero-coupon bond prices correspond to those observed in the market:

$$\theta(t) = \frac{1}{\kappa} \frac{\partial f^M(0, t)}{\partial t} + f^M(0, t) + \frac{\sigma^2}{2\kappa^2} (1 - e^{-2\kappa t}).$$

Hence, the market instantaneous forward rate curve is derived based on the observed prices of market bonds. In practice, this curve is often simplified by fitting a parametric function. The Nelson–Siegel–Svensson model [25] is widely adopted by central banks and financial practitioners for modeling the term structure of interest rates. In this framework, the market instantaneous forward rate at  $t = 0$  is expressed as:

$$f^M(0, T) = \beta_0 + \beta_1 e^{-\frac{T}{\tau_1}} + T \frac{\beta_2}{\tau_1} e^{-\frac{T}{\tau_1}} + T \frac{\beta_3}{\tau_2} e^{-\frac{T}{\tau_2}}, \quad (2.5)$$

where  $\beta_0, \beta_1, \beta_2, \beta_3, \tau_1$ , and  $\tau_2$  are parameters determined through market calibration. A major achievement in this field states that the short rate process  $r_t$  can be expressed as:

$$r_t = \omega R_t + \beta(t),$$

where  $R_t$  is a Vasicek process that evolves according to the following dynamics:

$$dR_t = -\kappa R_t dt + dW_t^r, \quad R_0 = 0, \quad (2.6)$$

and  $\beta(t)$  is a time-dependent function given by:

$$\beta(t) = f^M(0, t) + \frac{\omega^2}{2\kappa^2} (1 - e^{-\kappa t})^2. \quad (2.7)$$

In this framework, the price  $V(t, S_t, r_t)$  of a financial derivative with maturity  $T$  and payoff function  $\Psi(S_T)$  can be formulated as an optimization problem to account for volatility uncertainty. In particular, both the writer and the buyer of a financial derivative seek the worst-case volatility scenario to ensure robust pricing. Since any agent who has entered a short position on the contract fears the rise of the contract value, we specify the option price from such a perspective as

$$V^{Short}(t, S_t, r_t) = \sup_{\sigma \in [\sigma_{\min}, \sigma_{\max}]} \mathbb{E}^{\mathbb{Q}} \left[ e^{-\int_t^T r_u du} \Psi(S_T) \mid \mathcal{F}_t \right], \quad (2.8)$$

where  $\mathbb{E}^{\mathbb{Q}}$  denotes the expectation under  $\mathbb{Q}$  and  $\mathcal{F} = (\mathcal{F}_t)_{t \in [0, T]}$  represents the filtration generated by the processes  $S$  and  $r$ . Conversely, an economic agent who has assumed a long position on the derivative fears a drop in the contract price. For this reason, the value of the derivative is expressed as:

$$V^{Long}(t, S_t, r_t) = \inf_{\sigma \in [\sigma_{\min}, \sigma_{\max}]} \mathbb{E}^{\mathbb{Q}} \left[ e^{-\int_t^T r_u du} \Psi(S_T) \mid \mathcal{F}_t \right]. \quad (2.9)$$

These two formulations (2.8) and (2.9) ensure that the derivative price reflects the most adverse volatility scenario, yielding a conservative and robust valuation. The Hull-White model for  $r_t$  further introduces realistic interest rate dynamics, making this approach suitable for environments with both stochastic interest rates and uncertain volatility.

As far as an American contract is considered, we can identify three relevant formulations for the option price which take into account that the optimal exercise strategy is determined solely by the option buyer. Then, the price for the long agent is defined as follows:

$$V_{am}^{Long}(t, S_t, r_t) = \sup_{\tau \in \mathcal{T}} \inf_{\sigma \in [\sigma_{\min}, \sigma_{\max}]} \mathbb{E}^{\mathbb{Q}} \left[ \exp \left( -\int_t^\tau r_u du \right) \Psi(S_\tau) \mid \mathcal{F}_t \right], \quad (2.10)$$

where  $\mathcal{T}$  is the set of all stopping times with respect to the filtration  $\mathcal{F}$ . Let  $\tau_\star$  be the optimal stopping time, solving problem (2.10). As far as the short agent is considered, the price can be defined as follows, based on the stopping strategy  $\tau_\star$  followed by the buyer:

$$V_{am}^{Mix}(t, S_t, r_t) = \sup_{\sigma \in [\sigma_{\min}, \sigma_{\max}]} \mathbb{E}^{\mathbb{Q}} \left[ \exp \left( - \int_t^{\tau_*} r_u du \right) \Psi(S_{\tau_*}) \mid \mathcal{F}_t \right], \quad (2.11)$$

Finally, the writer may be interested in the maximum hedging cost of the option, which can be computed by assuming that the buyer does not choose the strategy that is most convenient for him but the strategy that is most expensive for the writer. This leads to the following formulation of the maximum option price for the short agent, which he should take into account for precautionary purposes, in case the buyer does not follow strategy  $\tau_*$ :

$$V_{am}^{Short}(t, S_t, r_t) = \sup_{\tau \in \mathcal{T}} \sup_{\sigma \in [\sigma_{\min}, \sigma_{\max}]} \mathbb{E}^{\mathbb{Q}} \left[ \exp \left( - \int_t^{\tau} r_u du \right) \Psi(S_{\tau}) \mid \mathcal{F}_t \right]. \quad (2.12)$$

### 3 The Tree UVHW method for option pricing

This Section presents a general version of the Tree UVHW algorithm, which can be applied to any European vanilla option. The algorithm employs two structures to discretize the market: a tree  $\mathcal{R}$  for the interest rate process  $R$  and a grid of representative values  $\mathcal{S}$  for the underlying equity index  $S$ . The values and transition probabilities are determined to match the first two moments of  $R$  and of  $\ln(S)$ , as well as their covariance. It should be noted that the tree structure for  $R$  is recombining in the sense that future values originating from a given node remain within the tree structure. In contrast, the lattice for  $S$  does not exhibit this characteristic, and linear interpolation is used to calculate conditional expectations at future time steps (a similar technique has been used by Costabile et al. [4] in a different insurance context). Additionally, the grid's ability to account for uncertainty in index volatility is advantageous, as it enables the management of different volatility values.

Before introducing the proposed pricing method in detail, we recall some properties of the Black-Scholes (BS) model with stochastic interest rate modeled by a Hull-White process.

**Proposition 1.** *Let  $R$  be the stochastic process defined in (2.6) and let  $W^S$  be a Brownian motion as in (2.1). Moreover, let  $I$  be the stochastic process representing the integral*

$$I_t = \int_0^t R_s ds.$$

*Then, for any time  $t > 0$  and time increment  $\Delta t > 0$ , the following relation holds:*

$$\begin{pmatrix} R_{t+\Delta t} - R_t \\ I_{t+\Delta t} - I_t \\ W_{t+\Delta t} - W_t \end{pmatrix} \mid R_t \sim \mathcal{N} \left( \begin{pmatrix} \mu_R \\ \mu_I \\ \mu_W \end{pmatrix}, \begin{pmatrix} \sigma_R^2 & \sigma_{R,I} & \sigma_{R,W} \\ \sigma_{R,I} & \sigma_I^2 & \sigma_{I,W} \\ \sigma_{R,W} & \sigma_{I,W} & \sigma_W^2 \end{pmatrix} \right)$$

with

$$\begin{aligned} \mu_R &= R_t (e^{-\kappa \Delta t} - 1), \quad \mu_I = -\frac{\mu_R}{\kappa}, \quad \mu_W = 0, \\ \sigma_R^2 &= \frac{1}{2\kappa} (1 - e^{-2\kappa \Delta t}), \quad \sigma_I^2 = \frac{1}{2\kappa^3} (2\kappa \Delta t + 4e^{-\kappa \Delta t} - e^{-2\kappa \Delta t} - 3), \quad \sigma_W^2 = \Delta t, \\ \sigma_{R,I} &= \frac{1}{2\kappa^2} (1 - e^{-\kappa \Delta t})^2, \quad \sigma_{R,W} = \frac{\rho}{\kappa} (1 - e^{-\kappa \Delta t}), \quad \sigma_{I,W} = \frac{\rho}{\kappa^2} (\kappa \Delta t + e^{-\kappa \Delta t} - 1). \end{aligned}$$

The proof of this key result is reported in Appendix A.

The Tree UVHW method for evaluating derivatives exploits lattice structures to discretize the stochastic processes that govern both the interest rate and the underlying asset index. This step involves dividing the

time interval between inception and maturity dates into  $N_T$  sub-intervals of equal length  $\Delta t$ . As a result,  $N_T = T/\Delta t$  represents the total number of time steps. Additionally, let  $t_n = n \cdot \Delta t$  a generic time step. Let us denote  $\bar{S} = \{\bar{S}_n\}_{n=0, \dots, N_T}$  and  $\bar{R} = \{\bar{R}_n\}_{n=0, \dots, N_T}$  the discrete time processes based used to approximate  $S$  and  $R$  respectively. In particular, the couple  $(\bar{S}_n, \bar{R}_n)$  approximates the couple  $(S_{t_n}, R_{t_n})$ .

The first step of the proposed algorithm is the construction of the tree structure for  $\bar{R}$ , which discretizes the interest rate dynamics. At each time step, the tree branches into several potential future states, capturing the possible evolution of the interest rate. The associated rate process  $\bar{R}$  at each tree node is updated using a discretized version of the Hull-White model's stochastic differential equation, ensuring that the tree remains recombining, meaning it merges into fewer states over time to enhance computational efficiency. Specifically, we employ the “multiple-jumps” tree introduced by Nelson and Ramaswamy [20] and further developed by Briani et al. in [2]. The lattice structure is as follows: for  $n = 0, 1, \dots, N_T$  we set

$$\mathcal{R}_n = \{\bar{R}_{n,j}\}_{j=0,1,\dots,n}, \quad \text{with } \bar{R}_{n,j} = (2j - n)\sqrt{\Delta t}.$$

For each fixed  $R_{n,j} \in \mathcal{R}_n$ , the “up” and “down” transitions value for  $\bar{R}_n = \bar{R}_{n,j}$  are

$$\bar{R}_{n+1}^{up}(j) = \bar{R}_{n+1,j_{up}(n,j)} \quad \text{and} \quad \bar{R}_{n+1}^{dw}(j) = \bar{R}_{n+1,j_{dw}(n,j)},$$

respectively. We stress out that both  $\bar{R}_{n+1}^{up}(j)$  and  $\bar{R}_{n+1}^{dw}(j)$  are elements of the set  $\mathcal{R}_{n+1}$ . The indices of these transitions,  $j_u(n, j)$  and  $j_d(n, j)$ , are defined as:

$$\begin{aligned} j_u(n, j) &= \min \{j^* \text{ s.t. } j+1 \leq j^* \leq n+1 \text{ and } \bar{R}_{n,j} + \mu_R(\bar{R}_{n,j}) \Delta t \leq \bar{R}_{n+1,j^*}\}, \\ j_d(n, j) &= \max \{j^* \text{ s.t. } 0 \leq j^* \leq j \text{ and } \bar{R}_{n,j} + \mu_R(\bar{R}_{n,j}) \Delta t \geq \bar{R}_{n+1,j^*}\}, \end{aligned}$$

where  $\mu_R(\bar{R}_{n,j}) = -\kappa \bar{R}_{n,j}$  represents the drift of  $R$ . Furthermore, if at time step  $n$  the process  $\bar{R}$  takes the value corresponding to the node  $(n, j)$ , the probability that the process  $\bar{R}$  moves to  $j_u(n, j)$  or to  $j_d(n, j)$  at time-step  $n+1$  are given by

$$p_{n,j}^{\bar{R},up} = 0 \vee \frac{\mu_R(\bar{R}_{n,j}) \Delta t + \bar{R}_{n,j} - \bar{R}_{n+1}^{dw}(j)}{\bar{R}_{n+1}^{up}(j) - \bar{R}_{n+1}^{dw}(j)} \wedge 1 \quad \text{and} \quad p_{n,j}^{\bar{R},dw} = 1 - p_{n,j}^{\bar{R},up}.$$

As far as the underlying is considered, we also exploit a lattice to discretize the process  $S$ . Usually, lattice methods for pricing, such as the CRR tree model [5] or the Jarrow Rudd model [18] require one to define the lattice based on the volatility of  $S$ , which is not possible in our case, since in UVM volatility is a single parameter, but a range of values  $[\sigma_{\min}, \sigma_{\max}]$ . In order to overcome this obstacle, the following approach is adopted. Since, the greater the value for  $\sigma$ , the greater the variance of the underlying, we define at each time step  $t_n$  the extreme values of the mesh for  $S$  based on  $\sigma_{\max}$  and on CRR model. In particular, we set

$$\bar{S}_n^{\max} = S_0 \exp(n\sigma_{\max}\sqrt{\Delta t}), \quad \bar{S}_n^{\min} = S_0 \exp(-n\sigma_{\max}\sqrt{\Delta t}).$$

We then define a uniform logarithmic mesh, denoted as  $\mathcal{S}_n$ , consisting of points evenly distributed on a logarithmic scale between  $\bar{S}_n^{\min}$  and  $\bar{S}_n^{\max}$ . The number of points used to define this mesh is an integer multiple of  $n+1$  which corresponds to the number of points at time-step  $t_n$  that would be obtained in the case of a binomial tree. Specifically, such a number is equal to  $N_S^n = N_S(n+1)$ , with  $N_S$  a large enough integer, thus

$$\mathcal{S}_n = \left\{ \bar{S}_{n,i} = S_0 \exp \left( \left[ \frac{2n}{N_S(n+1) - 1} (i-1) - n \right] \sigma_{\max} \sqrt{\Delta t} \right), \quad i = 1, \dots, N_S^n \right\}.$$

Furthermore, since the starting value of the discrete process  $\bar{S}$  coincides with that of the original continuous process  $S$ , we set

$$\mathcal{S}_0 = \{S_0\}.$$

Now, let us discuss how to define the transition dynamics of process  $\bar{S}$ , that is how to discretize the random variable  $(S_{t+\Delta t} \mid S_t, R_t, R_{t+\Delta t})$ . We begin this discussion by stating the following result.

**Proposition 2.** *The random variable  $(W_{t+\Delta t}^S - W_t^S \mid R_{t+\Delta t}, R_t)$  has the following probability distribution:*

$$(W_{t+\Delta t}^S - W_t^S \mid R_{t+\Delta t}, R_t) \sim \mathcal{N}(\mu_{W|R}, \sigma_{W|R}^2),$$

with

$$\mu_{W|R} = 2\rho \frac{1 - e^{-\kappa\Delta t}}{1 - e^{-2\kappa\Delta t}} (R_{t+\Delta t} - R_t e^{-\kappa\Delta t}), \quad \sigma_{W|R}^2 = \Delta t - 2\frac{\rho^2}{\kappa} \frac{1 - e^{-\kappa\Delta t}}{1 + e^{-\kappa\Delta t}}.$$

The proof of such a result is reported in Appendix B.

Now, let us focus on a particular market state, that is we consider  $(\bar{S}_n, \bar{R}_n) = (\bar{S}_{n,i}, \bar{R}_{n,j})$ . The possible future values for the rate process  $\bar{R}_{n+1}$  are  $\bar{R}_{n+1,j_u(n,j)}$  and  $\bar{R}_{n+1,j_d(n,j)}$ , respectively, as described above. For the time being, let us assume that, during the time interval  $[t_n, t_n + \Delta t]$ , the volatility of  $\bar{S}$  is constant, equal to a specific value  $\hat{\sigma} \in [\sigma_{\min}, \sigma_{\max}]$ . Generally speaking, we can observe that, if  $S_{t_n} = S_{n,i}$ , the solution of the SDE 2.1 in  $[t_n, T]$  reads out

$$S_u = S_{n,i} \exp \left( \int_{t_n}^u r_s ds - \left( \eta + \frac{\sigma^2}{2} \right) (u - t_n) + \sigma (W_u^S - W_{t_n}^S) \right) \quad (3.1)$$

for any  $u \in [t_n, T]$ . In particular, for  $u = t_{n+1}$ , we can write down

$$S_{t_{n+1}} = S_{n,i} \exp \left( \int_{t_n}^{t_{n+1}} r_s ds - \left( \eta + \frac{\sigma^2}{2} \right) \Delta t + \sigma (W_{t_{n+1}}^S - W_{t_n}^S) \right). \quad (3.2)$$

Therefore, to discretize the random value  $S_{t_{n+1}}$  given the future value  $R_{t_{n+1}}$ , that is  $\bar{R}_{n+1}$ , we develop the following approximation of the integral, based on the trapezoidal rule:

$$\int_{t_n}^{t_{n+1}} r_s ds = \omega \int_{t_n}^{t_{n+1}} R_s ds + \int_{t_n}^{t_{n+1}} \beta(s) ds \approx \omega \frac{\bar{R}_{n+1} + \bar{R}_n}{2} \Delta t + \int_{t_n}^{t_{n+1}} \beta(s) ds.$$

In this regard, note that the integral of the function  $\beta$  can be calculated exactly from the relations (2.7) and (2.5).

Furthermore, by exploiting Proposition 2, we replace the Gaussian random variable  $W_{t_{n+1}}^S - W_{t_n}^S$  with a discrete random variable  $H_n$  having the same first two moments:

$$H_n = \mu_{W|R} + \sqrt{\sigma_{W|R}} (2B - 1),$$

with  $B \sim \mathcal{B}(0.5)$  a Bernoulli's random variable independent from all the others. Moreover, let  $H^{up} = \mu_{W|R} + \sqrt{\sigma_{W|R}}$  be the value for  $H$  if  $B = 1$  and  $H^{dw} = \mu_{W|R} - \sqrt{\sigma_{W|R}}$  the value for  $H$  if  $B = 0$ . Based on the two possible values for  $\bar{R}_{n+1}$ , we replace the random variable  $(W_{t_{n+1}}^S - W_{t_n}^S \mid \bar{R}_{t_{n+1}}, \bar{R}_t)$  in (3.2) with  $H_n$ , so that there are four values for  $(\bar{S}_{n+1} \mid \bar{S}_n = \bar{S}_{n,i}, \bar{R}_n = \bar{R}_{n,j}, \bar{R}_{n+1})$ , namely  $\bar{S}_{n+1}^{up,up}(i,j)$ ,  $\bar{S}_{n+1}^{up,dw}(i,j)$  and  $\bar{S}_{n+1}^{dw,dw}(i,j)$ . Specifically, if  $\bar{R}_{n+1} = \bar{R}_{n+1}^{up}(j)$ , then

$$\bar{S}_{n+1}^{up,up}(i,j) = \bar{S}_{n,i} \exp \left( \omega \frac{\bar{R}_{n+1}^{up}(j) + \bar{R}_n}{2} \Delta t + \int_{t_n}^{t_{n+1}} \beta(s) ds - \left( \eta + \frac{\sigma^2}{2} \right) \Delta t + \sigma H^{up} \right), \quad (3.3)$$

$$\bar{S}_{n+1}^{up,dw}(i,j) = \bar{S}_{n,i} \exp \left( \omega \frac{\bar{R}_{n+1}^{up}(j) + \bar{R}_n}{2} \Delta t + \int_{t_n}^{t_{n+1}} \beta(s) ds - \left( \eta + \frac{\sigma^2}{2} \right) \Delta t + \sigma H^{dw} \right), \quad (3.4)$$



while if  $\bar{R}_{n+1} = \bar{R}_{n+1}^{dw}(j)$ , then

$$\bar{S}_{n+1}^{dw,up}(i,j) = \bar{S}_{n,i} \exp \left( \omega \frac{\bar{R}_{n+1}^{dw}(j) + \bar{R}_n}{2} \Delta t + \int_{t_n}^{t_{n+1}} \beta(s) ds - \left( \eta + \frac{\sigma^2}{2} \right) \Delta t + \sigma H^{up} \right), \quad (3.5)$$

$$\bar{S}_{n+1}^{dw,dw}(i,j) = \bar{S}_{n,i} \exp \left( \omega \frac{\bar{R}_{n+1}^{dw}(j) + \bar{R}_n}{2} \Delta t + \int_{t_n}^{t_{n+1}} \beta(s) ds - \left( \eta + \frac{\sigma^2}{2} \right) \Delta t + \sigma H^{dw} \right). \quad (3.6)$$

Moreover, in agreement with the probability distribution of  $B$ , the following equations hold:

$$\begin{aligned} \mathbb{Q}(\bar{S}_{n+1} = \bar{S}_{n+1}^{up,up}(i,j) \mid \bar{S}_n = \bar{S}_{n,i}, \bar{R}_n = \bar{R}_{n,j}, \bar{R}_{n+1} = \bar{R}_{n+1}^{up}(j)) \\ = \mathbb{Q}(\bar{S}_{n+1} = \bar{S}_{n+1}^{up,dw}(i,j) \mid \bar{S}_n = \bar{S}_{n,i}, \bar{R}_n = \bar{R}_{n,j}, \bar{R}_{n+1} = \bar{R}_{n+1}^{up}(j)) = \frac{1}{2} \end{aligned}$$

and

$$\begin{aligned} \mathbb{Q}(\bar{S}_{n+1} = \bar{S}_{n+1}^{dw,up}(i,j) \mid \bar{S}_n = \bar{S}_{n,i}, \bar{R}_n = \bar{R}_{n,j}, \bar{R}_{n+1} = \bar{R}_{n+1}^{dw}(j)) \\ = \mathbb{Q}(\bar{S}_{n+1} = \bar{S}_{n+1}^{dw,dw}(i,j) \mid \bar{S}_n = \bar{S}_{n,i}, \bar{R}_n = \bar{R}_{n,j}, \bar{R}_{n+1} = \bar{R}_{n+1}^{dw}(j)) = \frac{1}{2} \end{aligned}$$

As opposed to the two values for  $\bar{R}_{n+1}$  that belong to  $\mathcal{R}_{n+1}$ , the four values for  $\bar{S}_{n+1}$  may not belong to  $\mathcal{S}_{n+1}$ , but the use of one dimensional linear interpolation on  $\mathcal{S}_{n+1}$  allows one to overcome this obstacle. Specifically, one can use the previous definitions to compute discounted conditional expectation of a function  $f$  defined over the grid  $\mathcal{R}_{n+1} \times \mathcal{S}_{n+1}$ . To this aim, one has to extend  $f$  to  $\mathbb{R}^2$  by linear interpolation on  $\mathcal{R}_{n+1} \times \mathcal{S}_{n+1}$ , and then compute

$$\begin{aligned} \mathbb{E} \left[ \exp \left( - \int_{t_n}^{t_{n+1}} \omega R_s + \beta(s) ds \right) f(R_{t_{n+1}}, S_{t_{n+1}}) \mid R_{t_n} = \bar{R}_{n,j}, S_{t_n} = \bar{S}_{n,i} \right] \approx \\ \frac{1}{2} p_{n,j}^{\bar{R},up} d_n^{up}(j) \left[ f(\bar{R}_{n+1}^{up}(j), \bar{S}_{n+1}^{up,up}(i,j)) + f(\bar{R}_{n+1}^{up}(j), \bar{S}_{n+1}^{up,dw}(i,j)) \right] + \\ \frac{1}{2} p_{n,j}^{\bar{R},dw} d_n^{dw}(j) \left[ f(\bar{R}_{n+1}^{dw}(j), \bar{S}_{n+1}^{dw,up}(i,j)) + f(\bar{R}_{n+1}^{dw}(j), \bar{S}_{n+1}^{dw,dw}(i,j)) \right], \quad (3.7) \end{aligned}$$

with

$$\begin{aligned} d_n^{up}(j) &= \exp \left( -\omega \frac{\bar{R}_{n+1}^{up}(j) + \bar{R}_{n,j}}{2} \Delta t - \int_{t_n}^{t_{n+1}} \beta(s) ds \right), \\ d_n^{dw}(j) &= \exp \left( -\omega \frac{\bar{R}_{n+1}^{dw}(j) + \bar{R}_{n,j}}{2} \Delta t - \int_{t_n}^{t_{n+1}} \beta(s) ds \right), \end{aligned}$$

the discount factors from  $t_{n+1}$  to  $t_n$  in case of an up or down movement respectively. In particular, if we define

$$\begin{aligned} \bar{i}^{up,up}(i,j) &= \min \{ i^* \text{ s.t. } 1 \leq i^* \leq N_S^{n+1} \text{ and } \bar{S}_{n+1,i^*} \geq \bar{S}_{n+1}^{up,up}(i,j) \} \cup \{ N_S^{n+1} \}, \\ \underline{i}^{up,up}(i,j) &= \max \{ i^* \text{ s.t. } 1 \leq i^* \leq N_S^{n+1} \text{ and } \bar{S}_{n+1,i^*} \leq \bar{S}_{n+1}^{up,up}(i,j) \} \cup \{ 1 \}, \end{aligned}$$

then linear interpolation for  $f(\bar{S}_{n+1}^{up,up}(i,j), \bar{R}_{n+1}^{up}(j))$  writes down as

$$\begin{aligned} f(\bar{R}_{n+1}^{up}(j), \bar{S}_{n+1}^{up,up}(i,j)) &= \frac{\bar{S}_{n+1}^{up,up}(i,j) - \bar{S}_{n+1,\underline{i}^{up,up}(i,j)}}{\bar{S}_{n+1,\bar{i}^{up,up}(i,j)} - \bar{S}_{n+1,\underline{i}^{up,up}(i,j)}} f(\bar{R}_{n+1}^{up}(j), \bar{S}_{n+1,\bar{i}^{up,up}(i,j)}) \\ &\quad + \frac{\bar{S}_{n+1,\bar{i}^{up,up}(i,j)} - \bar{S}_{n+1}^{up,up}(i,j)}{\bar{S}_{n+1,\bar{i}^{up,up}(i,j)} - \bar{S}_{n+1,\underline{i}^{up,up}(i,j)}} f(\bar{R}_{n+1}^{up}(j), \bar{S}_{n+1,\underline{i}^{up,up}(i,j)}), \end{aligned}$$

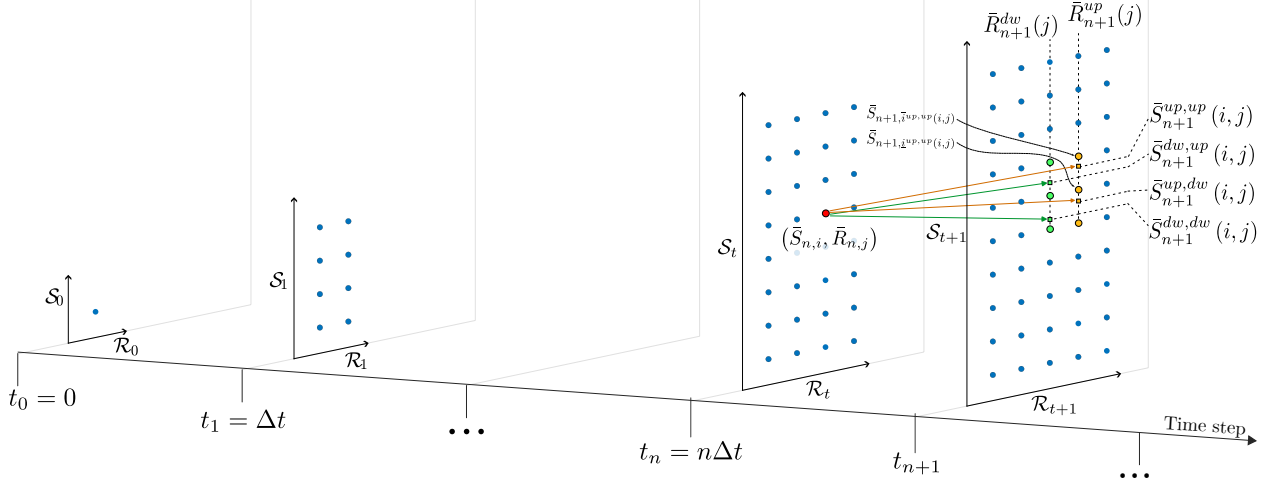


Figure 3.1: Structure of the nodes used by the Tree UVHW algorithm for evaluating a vanilla option.

where  $f(\bar{R}_{n+1}^{up}(j), \bar{S}_{n+1, \bar{i}^{up,up}}(i, j))$  and  $f(\bar{R}_{n+1}^{up}(j), \bar{S}_{n+1, \bar{i}^{up,up}}(i, j))$  are observable values since  $\bar{R}_{n+1}^{up}(j) \in \mathcal{R}_{n+1}$ ,  $\bar{S}_{n+1, \bar{i}^{up,up}} \in \mathcal{S}_{n+1}$  and  $\bar{S}_{n+1, \bar{i}^{up,up}} \in \mathcal{S}_{n+1}$ . In a similar manner, it is possible to compute linear interpolation for  $f(\bar{R}_{n+1}^{up}(j), \bar{S}_{n+1}^{up,dw}(i, j))$ ,  $f(\bar{R}_{n+1}^{dw}(j), \bar{S}_{n+1}^{dw,up}(i, j))$  and  $f(\bar{R}_{n+1}^{dw}(j), \bar{S}_{n+1}^{dw,dw}(i, j))$ .

Figure 3.1 summarizes the node structure and the backward procedure just described. In particular, the figure shows the structure of the nodes at initial time  $t_0$ , at time  $t_1$ , at a generic instant  $t_n$  and at its successor  $t_{n+1}$ . In addition, for a generic node  $(\bar{R}_{n,j}, \bar{S}_{n,i})$  at time  $t_n$  (see the red dot), the successor nodes (green and orange squares) and the grid nodes used for interpolation (green and orange dots) are highlighted.

On the whole, by applying Equation (3.7) backward in time, one can obtain the price of an European option in the Black-Scholes model with stochastic interest rate described by the Hull-White model.

Now, recall that in the UVM model, the value of  $\sigma$  is defined at each time instant  $t$ , for every market state  $S_t, R_t$ , in a way that optimizes the contract's continuation value. This is achieved by applying formula (3.7), where the function  $f$  represents the value of the contract being evaluated. Specifically, we solve the following optimization problem

$$\begin{aligned} \min/\max_{\sigma \in [\sigma_{\min}, \sigma_{\max}]} & \frac{1}{2} p_{n,j}^{\bar{R},up} d_n^{up}(j) \left[ f(\bar{R}_{n+1}^{up}(j), \bar{S}_{n+1}^{up,up}(i, j)(\sigma)) + f(\bar{R}_{n+1}^{up}(j), \bar{S}_{n+1}^{up,dw}(i, j)(\sigma)) \right] + \\ & \frac{1}{2} p_{n,j}^{\bar{R},dw} d_n^{dw}(j) \left[ f(\bar{R}_{n+1}^{dw}(j), \bar{S}_{n+1}^{dw,up}(i, j)(\sigma)) + f(\bar{R}_{n+1}^{dw}(j), \bar{S}_{n+1}^{dw,dw}(i, j)(\sigma)) \right], \end{aligned} \quad (3.8)$$

where the dependence of the future values  $\bar{S}_{n+1}^{up,up}(i, j)$ ,  $\bar{S}_{n+1}^{up,dw}(i, j)$ ,  $\bar{S}_{n+1}^{dw,up}(i, j)$  and  $\bar{S}_{n+1}^{dw,dw}(i, j)$  according to equation (3.3), (3.4), (3.5) and (3.6), is pointed out by writing  $\sigma$  in round brackets. Various numerical techniques can be employed to tackle this one-dimensional optimization problem. However, due to the lack of information on the uniqueness of the maximum, we opted for a straightforward grid search. In this approach, the objective function is evaluated at  $N_\sigma$  uniformly spaced points between  $\sigma_{\min}$  and  $\sigma_{\max}$ , and the best result is selected. Specifically, for  $N_\sigma = 2$ , only the endpoints of the interval  $\sigma_{\min}$  and  $\sigma_{\max}$  are used. Although this method is simple, it proves effective and empirical evidence suggests that the optimum frequently occurs at either  $\sigma_{\min}$  or  $\sigma_{\max}$ . In particular, when  $\rho = 0$ , it can be shown that the maximum coincides with one of these boundary values.

In conclusion, by solving problem (3.8) backward in time, one can obtain the price of an European option in the UVM with stochastic interest rate described by the Hull-White model.

*Remark 3.* The aforementioned procedure for the valuation of European options can be expanded to encompass the valuation of options with early exercise feature, such as Bermudian and American options. In particular, at each time step  $t_n$ , a comparison must be made between the continuation value and the exercise value of the option, with due care to distinguish between the possible Short, Long and Mixed approaches, as described in Section 2. We will describe this procedure in detail with reference to EIAs in the Section 4.

*Remark 4.* As a consequence of Proposition 1, also  $I_n = \int_{t_n}^{t_{n+1}} R_s ds$  is a Gaussian random variable correlated with  $R$  and  $W^S$ . Thus, one could have treated this integral as a Gaussian random variable to be discretized, as done for  $(W_{t_{n+1}}^S - W_t^S \mid \bar{R}_{t_{n+1}}, \bar{R}_t)$ . Since  $I_n$  appears in the definition of the future nodes for  $S_{t_{n+1}}$ , according to (3.2), this discretization would result in doubling the number of points at which the function  $f$  in (3.7) must be evaluated, thus increasing the computational cost of the algorithm. However, in the proposed implementation, such an integral has been discretized using the trapezoidal method. This technique proves to be more efficient from a numerical point of view. In fact, both the two ways of handling  $I_n$  have been implemented and the differences in the pricing results turns out to be less than 1‰. The discretization of the integral as a Gaussian random variable, on the other hand, increased the computation time by approximately 30% compared to the discretization using the trapezoidal rule.

## 4 The EIA contract

Let us discuss the structure of EIAs with cliquet-style guarantees under specific constraints, including the minimum contract value and the potential for early surrender. The contract description proposed in this paper is quite general and accommodates other more specific formulations, such as those proposed by Kijima and Wong [19], Wei et al. [27] and Cui et al. [6].

The contract is structured with periodic monitoring dates and spans  $T$  years, where  $T$  is an integer value. The payoff depends on the returns of the equity index at predetermined uniformly distributed time points  $\{\tilde{t}_m = m\frac{T}{M}, m = 0, \dots, M\}$  between  $t = 0$  and  $t = T$ . Therefore, the periodic linear return  $Y_m$  of the underlying index in  $[\tilde{t}_{m-1}, \tilde{t}_m]$  reads out

$$Y_m = \frac{S_{\tilde{t}_m}}{S_{\tilde{t}_{m-1}}} - 1, \quad m = 1, \dots, M.$$

For each period, the returns are adjusted using a local cap  $C_l$  and floor  $F_l$ . Additionally, the cumulative return across all periods is subject to a global cap  $C_g$  and a floor  $F_g$ . The resulting value is added to a running total. In this regard, we define the discrete time processes  $Z = (Z_m)_{m \in \{0, \dots, M\}}$  and  $X = (X_m)_{m \in \{0, \dots, M\}}$  as follows:

$$Z_m = \sum_{j=1}^m \max(F_l, \min(C_l, Y_j)), \quad Z_0 = 0, \quad (4.1)$$

$$X_m = K[H + \max(F_g, \min(C_g, Z_m))], \quad (4.2)$$

where  $K > 0$  is a notional value and  $H$  can be either 1 or 0 depending on the contract formulation. In particular, the scope of  $H$  is to determine the basis of contract formulation, whether that be net return or gross return. Please, observe that the cumulative sum  $Z$  reflects the growth of the annuity over time, incorporating the effects of local caps and floors on the periodic returns. In contrast,  $X$  captures the impact of global caps and floors applied to the cumulative return. A global minimum contract value (MCV), defined as

$$G_m = \gamma \left[ (1 + g)^{\tilde{t}_m} + 1 - H \right], \quad (4.3)$$

ensures that the payoff the  $m$ -th monitoring date cannot fall below  $G_m$ . More specifically,  $g \geq 0$  represents the guaranteed minimum rate, and  $\gamma$  is a fraction of the initial premium. In particular, the payoff at maturity is given by:

$$\Psi(X_T, G_T) = \max(X_T, G_T). \quad (4.4)$$

Incorporating an early surrender option allows the policyholder to terminate the contract at specific monitoring dates, if it is considered financially advantageous. In this case, at monitoring date  $m$ , the policyholder can either continue the contract or surrender to receive a payoff equal to the greater between the accumulated value  $Z_m$  and the corresponding minimum contract value, that is

$$\Psi(X_m, G_m) = \max(X_m, G_m).$$

In practice, early surrender often incurs charges that decrease over time. For example, a surrender penalty  $\xi(m, N_c)$  may apply, which usually depends on  $N_c$ , that is the number of periods the penalty is active. In this particular instance, the payoff in such cases reads out:

$$\Psi(m, X_m, G_m) = \max((1 - \xi(m, N_c)) X_m, G_m). \quad (4.5)$$

We stress out that the valuation of the EIAs contract with MCV, as described above, involves pricing a Bermudan path-dependent contingent claim within a continuous bivariate stochastic model. For this reason, it is necessary to use a specially designed numerical algorithm, such as the one described in the next Section.

*Remark 5.* Comparing with the literature on this topic, we can observe that the contract investigated by Kijima and Wong [19] and by Wei et al. [27] can be obtained by setting  $K = 1$ ,  $H = 1$  and  $F_g = -\infty$ ,  $C_g = +\infty$ . Moreover, the contract discussed by Cui et al. [6] can be obtained by setting  $H = 0$  and  $\gamma = 1$ .

## 5 The Tree UVHW method for EIAs

Let us discuss how to adapt the Tree UVHW algorithm to the evaluation of an EIA contract. First, we recall that, as explained in Section 4, the contract's lifespan is divided into  $M$  periods at the end of which the value of the underlying equity index  $S$  is observed. For the sake of simplicity, we assume an annual monitoring frequency, though other frequencies, such as monthly, may also be considered. Under this assumption, monitoring dates align with the contract's anniversary, that is  $\tilde{t}_m = m$ , and their total number  $M$  equals  $T$ .

We divide each period  $[m, m+1]$  into  $N_L$  (local) sub periods, each of duration  $\Delta t = 1/N_L$ , so that  $N_T = N_L M$  is the total number of discretization steps from contract inception to maturity time  $T$  and  $T = N_T \Delta t$ . Since  $N_L$  is an integer, the monitoring dates  $m = 1, \dots, M$  are naturally included within the algorithm time steps.

The procedure leverages both local and global structures to exploit the geometric properties of the contract under consideration, thereby reducing the computational complexity of the problem. Specifically, we define a structure as *global* if it extends temporally from the initial time  $t = 0$  to maturity  $t = T$ . Conversely, we define a structure as *local* if it extends temporally between two price monitoring dates,  $m$  and  $m+1$ .

The first global structure we consider is the tree  $\mathcal{R} = \{\mathcal{R}_n, n = 0, \dots, N_T\}$ , which is employed to discretize the process  $R$  through the discrete time process  $\bar{R}$ , from  $t = 0$  and  $t = T$  with  $N_T$  time steps and time increment  $\Delta t$ . Such a tree is built as described in Section 3.

Then, we define a global structure  $\mathcal{Z} = \{\mathcal{Z}_m, m = 0, \dots, M\}$ , which is employed to discretize the process  $Z$  from  $t = 0$  and  $t = T$  with  $M$  time steps and time increment 1 year. Specifically, we define a grid

$Z_m = \{Z_{m,k}\}_{k=1,\dots,N_Z}$  of values for the process  $Z$  for each monitoring date  $m = 1, \dots, M$ . Such a grid consists of a set of  $N_Z$  values uniformly distributed between  $Z_{m,1} = mF_l$  and  $Z_{m,N_Z} = mC_l$ , that is, the minimum and maximum possible values for  $Z_m$ , respectively. In addition, we set  $Z_0 = \{Z_{0,1} = 0\}$ .

The third structure we employ is a local grid  $\mathcal{S} = \{S_h, h = 0, \dots, N_L\}$ , which is used to discretize the process  $S$  through the discrete time process  $\bar{S}$ , between two monitoring dates  $m$  and  $m+1$ , with  $N_L$  time steps per period and time increment  $\Delta t$ . This structure  $\mathcal{S}$  serves to keep track of the local evolution of the equity index  $S$ . In particular, the values  $S_m$  and  $S_{m+1}$  determine the return over the period and thus the new values  $Z_{m+1}$  as follows

$$Z_{m+1} = Z_m + \max \left( F_l, \min \left( C_l, \alpha \left( \frac{S_{m+1}}{S_m} - 1 \right) \right) \right).$$

Therefore, knowledge of  $Z_{m+1}$  is sufficient to determine the exercise value of the option at the  $(m+1) - th$  monitoring date, that is

$$\Psi(m+1, K[H + \max(F_g, \min(C_g, Z_{m+1}))], G_{m+1}).$$

Moreover, since the law of the return  $(S_{m+1}/S_m - 1 \mid S_m = s)$  is the same of  $(S_{m+1} - 1 \mid S_m = 1)$ , we can write

$$Z_{m+1} \sim Z_m + \max(F_l, \min(C_l, \alpha(S_{m+1} - 1))).$$

Thus, the process  $Z$  is Markovian: it is possible to obtain  $Z_{m+1}$  from  $Z_m$  and  $(S_{m+1} \mid S_m = 1)$ .

At each monitoring date  $m$ , that is at time step  $mN_L$ , the contract value is uniquely determined by the values of processes  $Z_m$  and  $R_m$ , whereas at an intermediate time  $t_n = n\Delta t$ , such that  $m < t_n < m+1$ , the contract value is uniquely determined by the values of processes  $Z_m$ ,  $R_{t_n}$ , and  $(S_{n\Delta t} \mid S_m = 1)$ . Accordingly, for each value  $Z_{m,k}$  in  $\mathcal{Z}_m$ , we build the tree structure  $\mathcal{S}$  to discretize the underlying process between monitoring dates  $m$  and  $m+1$  under the assumption  $S_m = 1$ , therefore  $\mathcal{S}_0 = \{1\}$ . Such a structure is built as described in Section 3.

To describe the price of a contract, as approximated by the proposed method, we use two distinct families of pricing functions: a local one and a global one. Let us denote with  $V_m^{glo}$  the approximation of the contract price at the  $m$ -th monitoring date (in particular, the superscript *glo* stands for *global*). Such a function depends on the cumulative return process  $Z$  and on the discrete rate process  $\bar{R}$ :

$$V_m^{glo} = V_m^{glo}(Z_{m,k}, \bar{R}_{mN_L,j}), \quad Z_{m,k} \in \mathcal{Z}_m, \bar{R}_{mN_L,j} \in \mathcal{R}_{mN_L}.$$

We also consider a family of local functions, denoted by  $V_{m,h,k}^{loc}$ , determined under the assumption  $Z_m = Z_{m,k} \in \mathcal{Z}_m$ , to represent the contract price between two monitoring dates, say at time  $t_n = n\Delta t$  in the time interval  $[m, m+1]$  (in particular, the superscript *loc* in  $V_{m,h,k}^{loc}$  stands for *local*). In particular,  $m = \lfloor n/N_L \rfloor$  is the monitoring date immediately before time  $t_n = n\Delta t$ , and  $h$  is the remainder of the division of  $n$  by  $N_L$ , so that we write  $n = mN_L + h$ . Please, observe that each of these functions  $V_{m,h,k}^{loc}$  is identified by the observation time  $m$ , the number of (sub)-steps  $h$  after monitoring date  $m$ , and by  $k$  the index of the value  $Z_{m,k} \in \mathcal{Z}_m$  taken by the process  $Z$  at the  $m$ -th monitoring date. Each function  $V_{m,h,k}^{loc}$  depends on the discrete processes  $\bar{R}$  and  $\bar{S}$  at the  $n - th$  time step:

$$V_{m,h,k}^{loc} = V_{m,h,k}^{loc}(\bar{R}_{n,j}, \bar{S}_{h,i}), \quad h \in \{0, 1, \dots, N_L\}, \bar{R}_{n,j} \in \mathcal{R}_n, \bar{S}_{h,i} \in \mathcal{S}_h.$$

Let us now discuss how these functions interact with each other. At maturity, we observe that the value of  $V_M^{glo}$  can be deduced by the payoff function by setting

$$V_T^{glo}(Z_{M,k}, \bar{R}_{N_T,j}) = \Psi(T, K[H + \max(F_g, \min(C_g, Z_{M,k}))], G_T).$$

Then, let us assume that the function  $V_{m+1}^{glo}$  is known. In order to compute  $V_m^{glo}$ , we exploit  $V_{m,h,k}^{loc}$ . Specifically, for all  $k = 1, \dots, N_Z$ , we set

$$V_{m,N_L,k}^{loc}(\bar{R}_{n,j}, \bar{S}_{h,i}) = V_{m+1}^{glo}(Z_{m,k} + \max(F_l, \min(C_l, \alpha(\bar{S}_{h,i} - 1))), \bar{R}_{n,j}). \quad (5.1)$$

Please, observe that equation (5.1) is pivotal in establishing a connection between the global and local problems. If the value  $Z_{m,k} + \max(F_l, \min(C_l, \alpha(\bar{S}_{h,i} - 1)))$  is not included among the values of  $\mathcal{Z}_{m+1}$ , then linear interpolation of  $V_{m+1}^{glo}$  over  $\mathcal{Z}_{m+1} \times \mathcal{R}_{(m+1)N_T}$  is used.

Now, let us assume that the function  $V_{m,h+1,k}^{loc}$  is known and let us discuss how to compute  $V_{m,h,k}^{loc}$ . We focus on a particular node of the tree, that is  $(\bar{R}_{n,j}, \bar{S}_{h,i}) \in \mathcal{R}_n \times \mathcal{S}_h$ . We compute  $V_{m,h,k}^{loc}(\bar{R}_{n,j}, \bar{S}_{h,i})$  as the solution of the optimization problem (5.2) where  $f$  is replaced by  $V_{m,h+1,k}^{loc}$ , that is

$$\begin{aligned} \min/\max_{\sigma \in [\sigma_{\min}, \sigma_{\max}]} & \frac{1}{2} p_{n,j}^{\bar{R},up} d_n^{up}(j) \left[ V_{m,h+1,k}^{loc}(\bar{R}_{n+1}^{up}(j), \bar{S}_{h+1}^{up,up}(i,j)(\sigma)) + V_{m,h+1,k}^{loc}(\bar{R}_{n+1}^{up}(j), \bar{S}_{h+1}^{up,dw}(i,j)(\sigma)) \right] + \\ & \frac{1}{2} p_{n,j}^{\bar{R},dw} d_n^{dw}(j) \left[ V_{m,h+1,k}^{loc}(\bar{R}_{n+1}^{dw}(j), \bar{S}_{h+1}^{dw,up}(i,j)(\sigma)) + V_{m,h+1,k}^{loc}(\bar{R}_{n+1}^{dw}(j), \bar{S}_{h+1}^{dw,dw}(i,j)(\sigma)) \right] \end{aligned} \quad (5.2)$$

where  $V_{m,h+1,k}^{loc}$  is extended by linear interpolation over  $\mathcal{R}_{n+1} \times \mathcal{S}_{h+1}$ .

We highlight that in (5.2), the minimum operator is applied when analyzing a long position on the contract, while the maximum operator is used for a short position. Solving problems (5.2) iteratively, backward in time, we are able to obtain  $V_{m,0,k}^{loc}$  on  $\mathcal{R}_{mN_L} \times \mathcal{S}_0$ , where we underline again  $\mathcal{S}_0 = \{1\}$ . Finally, we set

$$V_m^{glo}(Z_{m,k}, \bar{R}_{mN_L,j}) = V_{m,0,k}^{loc}(\bar{R}_{mN_L,j}, 1), \quad Z_{m,k} \in \mathcal{Z}_m, \bar{R}_{mN_L,j} \in \mathcal{R}_{mN_L}. \quad (5.3)$$

Please note that Equation (5.3) acts as a link, thereby enabling the intermediate solution of the global problem to be obtained from the final solution of the local problem. This procedure, replicated iteratively from monitoring date  $m = M$  to  $m = 0$ , allows the value of the European contract to be calculated back in time to the initial time  $t = 0$ . Thus, the value of the contract at inception is approximated by  $V_0^{glo}(0,0)$ .

Furthermore, if the contract permits early surrender, the contract value at any monitoring date  $m$  is defined as the maximum between the continuation value  $\mathcal{C}_m$  and the exercise value  $\mathcal{E}_m$ . In this regard, we replace Equation (5.3) with the following one:

$$V_m^{glo}(Z_{m,k}, \bar{R}_{n,j}) = \max(\mathcal{C}_m(Z_{m,k}, \bar{R}_{n,j}), \mathcal{E}_m(Z_{m,k})), \quad (5.4)$$

with

$$\mathcal{C}_m(Z_{m,k}, \bar{R}_{n,j}) = V_{m,0,k}^{loc}(\bar{R}_{n,j}, 1) \quad (5.5)$$

$$\mathcal{E}_m(Z_{m,k}) = \Psi(m, K[H + \max(F_g, \min(C_g, Z_{m,k}))], G_m). \quad (5.6)$$

Equation (5.4) holds when we assume a pure long or a pure short position, that is when we aim to compute  $V_{am}^{Long}$  or  $V_{am}^{Short}$  respectively. In contrast, when a mixed position is considered, we consider operator  $\max$  in (5.2) and we replace (5.4) with

$$\begin{aligned} V_m^{glo}(Z_{m,k}, \bar{R}_{n,j}) &= \mathcal{C}_m^{Short}(Z_{m,k}, \bar{R}_{n,j}) \mathbb{1}_{\mathcal{C}_m^{Long}(Z_{m,k}, \bar{R}_{n,j}) > \mathcal{E}_m(Z_{m,k})} \\ &+ \mathcal{E}_m(Z_{m,k}) \mathbb{1}_{\mathcal{C}_m^{Long}(Z_{m,k}, \bar{R}_{n,j}) \leq \mathcal{E}_m(Z_{m,k})}, \end{aligned} \quad (5.7)$$

that is, we apply the optimal exercise strategy of the long position jointly with the contract value maximization provided by the UVM for the short position.

*Remark 6.* If the contract provides for non-annual monitoring dates, the procedure described in this Section remains valid, with the only caveat that, instead of dividing the year into  $N_L$  sub-periods, the period between two consecutive monitoring dates  $[\tilde{t}_{m-1}, \tilde{t}_m]$  will be divided, accordingly.

## 6 The GTU algorithm for EIAs

To assess the performance of the proposed algorithm, we compare it with a well-established algorithm. Due to the limited literature in this field, we have selected another tree-based algorithm, the Gaussian Process Regression - Tree for the UVM model (GTU), introduced by Goudenège et al. [10]. Originally developed for the multidimensional UVM model, this algorithm is particularly effective in pricing options on multiple underlyings, each modeled by UVM with uncertain correlations. However, GTU can be adapted to price EIAs within the stochastic interest rate UVM framework considered in this study and here we explain how to adapt this algorithm for our purpose.

The UVM algorithm operates backward in time, starting from the contract's maturity and progressing to the initial time. At each time step, it computes the contract's price for each point on a random grid by determining the continuation value as the expected discounted value of the contract at the subsequent time step, using a tree-based procedure. To extend the contract's value from the grid to the entire space, the algorithm employs Gaussian Process Regression (GPR), a machine learning technique that derives an approximating function from observed values on scattered points.

Let us now go into the details of the GTU algorithm for pricing EIAs. As in the previous Section 3, the valuation algorithm will be described assuming an annual revaluation basis for the contract. Using the same notation, we consider a number  $N_L$  of time steps per contract period, so that  $N_T = N_L M$  is the total number of discretization steps. As usual,  $\Delta t = 1/N_L$  is the time interval between two time steps of the algorithm. The algorithm starts by defining a stochastic grid of values for each time step, which will subsequently be utilized for computing the GPR. Therefore, we consider a set of  $N_{MC}$  Monte Carlo paths for the market variables  $(S, R, I)$ , sampled using a time discretization step equal to  $\Delta t$ , which we denote with

$$\{(S_n^i, R_n^i, I_n^i), n = 0, \dots, N_T, i = 1, \dots, N_{MC}\}.$$

This indicates that  $S_n^i$  represents the specific  $i$ -th simulated value of  $S_{n\Delta t}$  and the same applies to the other market variables. Such a simulation can be easily performed by considering the algorithm described in Goudenège et al. [9] for the Black-Scholes Hull-White model once a particular value for the volatility  $\sigma$  is considered. In particular, at each time step, we exploit Proposition 1 to simulate the Gaussian random variables  $(R_{(n+1)\Delta t} - R_{n\Delta t} \mid R_{n\Delta t} = R_n^i)$ ,  $(I_{(n+1)\Delta t} - I_{n\Delta t} \mid R_{n\Delta t} = R_n^i)$  and  $W_{(n+1)\Delta t}^S - W_{n\Delta t}^S$ , and then we set

$$\begin{aligned} R_{n+1}^i &= (R_{(n+1)\Delta t} - R_{n\Delta t}) + R_n^i, \\ S_{n+1}^i &= S_n^i \exp \left( (I_{(n+1)\Delta t} - I_{n\Delta t}) - \left( \eta + \frac{\sigma^2}{2} \right) \Delta t + \sigma (W_{(n+1)\Delta t}^S - W_{n\Delta t}^S) \right). \end{aligned}$$

Since in UVM  $\sigma$  is constrained in the range  $[\sigma_{\min}, \sigma_{\max}]$ , we address the lack of knowledge on such a parameter by splitting the set of simulations into two equally sized subgroups; half of the trajectories are simulated using  $\sigma = \sigma_{\min}$ , while the other half are simulated using  $\sigma = \sigma_{\max}$ . After running these simulations, for each monitoring date  $m$  we compute the respective value for process  $Z$ , that is

$$Z_m^i = \sum_{j=1}^m \max \left( F_l, \min \left( C_l, \alpha \left( S_{mN_L}^i / S_{(m-1)N_L}^i - 1 \right) \right) \right), \quad Z_0^i = 0.$$

At each time step, we utilize these random simulations to discretize the market state into a set  $\mathcal{X}_n$  of specific points. In particular, let us write  $n = mN_L + h$  with  $m = \lfloor n/N_L \rfloor$  the monitoring date immediately before time  $t = n\Delta t$ , and  $h$  the remainder of the division of  $n$  by  $N_L$ . Let us distinguish between two cases: if  $n\Delta t$  is a monitoring date, that is if  $h = 0$  and  $n = mN_L$ , then the EIAs price depends only on  $Z_{n\Delta t}$  and on  $R_{n\Delta t}$ . The set designed to illustrate the potential states of the market is

$$\mathcal{X}_m^{glo} = \{(Z_m^i, R_{mN_L}^i), i = 1, \dots, N_{MC}\}. \quad (6.1)$$

On the contrary, if the considered time step is not a monitoring date, that is if time  $t_n = n\Delta t$  is between two monitoring dates, then the EIAs price depends on  $Z_{n\Delta t}$ ,  $S_{n\Delta t}/S_m$  and on  $R_{n\Delta t}$ , so we define

$$\mathcal{X}_n^{loc} = \{(Z_m, S_n^i/S_{mN_L}^i, R_n^i), i = 1, \dots, N_{MC}\}. \quad (6.2)$$

The GTU algorithm computes the contract value backward in time, starting from maturity up to inception. The key elements of this algorithm are the calculation of continuation values using a tree method and the use of GPR to ensure that the contract price can also be calculated from points representing possible market states. Similar to the UVHW algorithm, we consider both global and local value functions. As in the previous Section 3, let us denote  $V_m^{glo} = V_m^{glo}(Z_m^i, R_{mN_L}^i)$  the approximation of the contract price at the  $m$ -th monitoring date for  $m \in \{0, \dots, M\}$ . We also consider a family of functions, denoted by  $V_{m,h}^{loc} = V_{m,h}^{loc}(Z_m, S_n^i/S_{mN_L}^i, R_n^i)$ , that represent the contract price between two monitoring dates, that is at the  $n - th$  time step with  $n = mN_L + h$  for  $m \in \{0, \dots, M\}$  and  $h \in \{0, \dots, N_L - 1\}$ .

The contract value at maturity is given by the payoff function  $\Psi$ , so we set

$$V_T^{glo}(Z_M^i, R_{N_T}^i) = \Psi(T, K[H + \max(F_g, \min(C_g, Z_M^i))], G_T).$$

Then, let us assume that the function  $V_{m+1}^{glo}$  is known. In order to compute  $V_m^{glo}$ , we exploit  $V_{m,h}^{loc}$ . First of all let us explain how to compute  $V_{m,N_L-1}^{loc}$  from  $V_{m+1}^{glo}$ , so let us assume  $n = (m+1)N_L - 1$ . The calculation of  $V_{m,N_L-1}^{loc}$  for all points in  $\mathcal{X}_n^{loc}$  requires computing the  $\sigma$  value that optimized the continuation value, that is a conditional expectation. Such an expectation is estimated by discretizing the possible market states at next time step by exploiting Proposition 1. Specifically, let be  $C$  the Cholesky lower factorization of covariance matrix in Proposition 1. We discretize the possible Gaussian variations of  $R, I$  and  $W^S$ , that is

$$(\Delta R_k = R_{(n+1)\Delta t} - R_{n\Delta t} \mid R_{n\Delta t} = R_n^i), (\Delta I_k = I_{(n+1)\Delta t} - I_{n\Delta t} \mid R_{n\Delta t} = R_n^i), (\Delta W_k = W_{(n+1)\Delta t}^S - W_{n\Delta t}^S)$$

with eight equiprobable values  $\Delta R_k, \Delta I_k, \Delta W_k$ ,  $k = 1, \dots, 8$  defined as

$$\begin{pmatrix} \Delta R_k \\ \Delta I_k \\ \Delta W_k \end{pmatrix} = \begin{pmatrix} \mu_R \\ \mu_I \\ \mu_W \end{pmatrix} + Cg_k,$$

being  $g_k$  the  $k$ -th element of the space  $\{-1, +1\}^3$ , for  $k = 1, \dots, 8$ . Thus, for each point in  $\mathcal{X}_n^{loc}$ , we set

$$V_{m,N_L-1}^{loc}(Z_m, S_n^i/S_{mN_L}^i, R_n^i) = \min/\max_{\sigma \in [\sigma_{\min}, \sigma_{\max}]} \frac{1}{8} \sum_{k=1}^8 e^{-\Delta I_k - \int_{t_n}^{t_{n+1}} \beta(s) ds} V_{m+1}^{glo}(Z_{m+1}^{i,k}, R_{n+1}^{i,k}) \quad (6.3)$$

with

$$R_{n+1}^{i,k} = R_n^i + \Delta R_k$$

and

$$Z_{m+1}^{i,k} = Z_m + \max(F_l, \min(C_l, \alpha(S_n^{i,k}(\sigma)/S_{mN_L}^i - 1))),$$



being

$$S_{n+1}^{i,k}(\sigma) = S_n^i \exp \left( \Delta I_k + \int_{t_n}^{t_{n+1}} \beta(s) ds - \eta \Delta t - \frac{\sigma^2}{2} \Delta t + \sigma \Delta W_k \right). \quad (6.4)$$

It is important to observe that in (6.3), the points  $(Z_{m+1}, R_{n+1}^{i,1}), \dots, (Z_{m+1}, R_{n+1}^{i,8})$  at which the function  $V_{m+1}^{glo}$  is evaluated do not belong to  $\mathcal{X}_{m+1}^{glo}$  almost sure, so one need to extend  $V_{m+1}^{glo}$ . This is done by using the GPR, a powerful Bayesian machine learning technique used for regression tasks. The reader is referred to Rasmussen and Williams [22] for more information on GPR. Specifically, the GPR model is trained using  $\mathcal{X}_{m+1}^{glo}$  as the predictor set and  $\mathcal{Y}_{m+1}^{glo} = \{V_{m+1}^{glo}(Z_{m+1}^i, R_{n+1}^i), m = 1, \dots, M\}$  as the target set. Finally, as done for Tree UVHW in Section (3), we solve the optimization problem in (6.3) by evaluating at  $N_\sigma$  uniformly spaced points between  $\sigma_{\min}$  and  $\sigma_{\max}$ , and the best result is selected.

Now, let us assume that the function  $V_{m,h+1}^{loc}$  is known, and let  $n = mN_L + h$ . The calculation of  $V_{m,h}^{glo}$  is developed following a similar approach to the one devised in (6.3). Specifically, for each point in  $\mathcal{X}_n^{loc}$ , we set

$$V_{m,h}^{glo}(Z_m^i, S_n^i/S_{mN_L}^i, R_n^i) = \min/\max_{\sigma \in [\sigma_{\min}, \sigma_{\max}]} \frac{1}{8} \sum_{k=1}^8 e^{-\Delta I_k - \int_{t_n}^{t_{n+1}} \beta(s) ds} V_{m,h+1}^{loc} \left( Z_m^i, S_{n+1}^{i,k}(\sigma)/S_{mN_L}^i, R_{n+1}^{i,k} \right), \quad (6.5)$$

The points  $(Z_m^i, S_{n+1}^{i,1}(\sigma)/S_{mN_L}^i, R_{n+1}^{i,1}), \dots, (Z_m^i, S_{n+1}^{i,8}(\sigma)/S_{mN_L}^i, R_{n+1}^{i,8})$  at which the function  $V_{m,h+1}^{loc}$  is evaluated do not belong to  $\mathcal{X}_n^{loc}$  almost sure, so we exploit again GPR. Specifically, a GPR model is trained using  $\mathcal{X}_{n+1}^{loc}$  as the predictor set and  $\mathcal{Y}_{n+1}^{loc} = \{V_{m,h+1}^{loc}(Z_m^i, S_{n+1}^i/S_{mN_L}^i, R_{n+1}^i), i = 1, \dots, N_{MC}\}$  as the target set.

Solving problems (6.5) iteratively, backward in time, we are able to obtain  $V_{m,0}^{loc}$  for all points in  $\mathcal{X}_{mN_L}^{loc}$ . Finally, we define  $V_m^{glo}$  on  $\mathcal{X}_m^{glo}$  by setting

$$V_m^{glo}(Z_m^i, R_{mN_L}^i) = V_{m,0}^{loc}(Z_m^i, 1, R_{mN_L}^i) \quad (6.6)$$

for all points in  $\mathcal{X}_m^{glo}$ .

Finally, it is important to note that the contract under consideration may include a surrender option. In this case, the relevant price will be defined by comparing the exercise value with the continuation value, with appropriate distinctions made between the Long, Short and Mix formulations discussed in Section 2. The relevant formulae can be obtained by adapting the corresponding (5.5), (5.6) and (5.7) developed for the Tree UVHW algorithm.

## 7 Numerical experiments

This Section presents the results of numerical experiments conducted to evaluate the performance of the proposed algorithm under various conditions. In the initial series of tests, the present study evaluates a contract that is equivalent in parameters to that analyzed in the recent paper by Cui et al. [6]. The objective of the present study is to emphasize the substantial contribution of the UVM model and the Hull-White model to the evaluation of contracts with cliquet-type clauses. In this initial phase of the investigation, the effects of uncertain volatility and the stochastic rate are considered separately. In a subsequent phase, however, the joint effect of these two elements is studied. For the latter, the insurance product treated by Kijima and Wong [19] is taken as a point of reference. The numerical convergence of the Tree UVHW

algorithm is analyzed, after which the valuation of contracts with early surrender option is studied in detail, with particular attention paid to the optimal exercise strategy in relation to the model assumptions.

The evaluation of the EIAs contacts is primarily conducted through the utilization of the Tree UVHW algorithm. The outcomes of this evaluation are then compared with those derived via the GTU algorithm. In instances where feasible, we have additionally presented prices derived through Monte Carlo simulations, which function as benchmarks. All numerical procedures were implemented in Matlab, and the calculations were performed on a PC with 16GB RAM and an Intel Ultra 5 125H processor.

## 7.1 Investigating the impact of uncertain volatility on EIAs price

In this sub Section we discuss the disjointed impact of uncertain volatility under constant interest rate. In this study, the same contract that was recently examined by Cui et al. [6] under a regime switch model is considered once more. The analysis commences with a focus on the UVM model, excluding the stochastic rate. This approach involves the cancellation of rate volatility and the assumption of a flat curve for ZCB prices. In particular, we compare the result of the BS model with both minimum and maximum prices returned by the UVM, to highlight the contribution of uncertain volatility. The parameters that serve to identify both the contract and the model are enumerated in Table 1. Moreover, the contract provides for monitoring dates on a monthly rather than annual basis. We stress out that these parameters align precisely with those used in [6]. It is important to highlight that, for this contract, the returns are computed on a monthly basis. The resulting graphs are displayed in Figure 7.1. Specifically, the left panel illustrates the price as a function of  $\sigma$ , while the right panel shows the variation with respect to  $C_l$ . The results are noteworthy for two key reasons. First, they demonstrate that in UVM, the contract price is no longer a single fixed value but rather a range of possible values. The price derived from the BS model falls within this range, and more broadly, the price is influenced by the evaluator perspective. Secondly, in contrast to what was observed in Figures 4 and 6 in [6] and remarked by the authors, the price does not collapse into a single value either for high values of  $\sigma$  or for relatively small values of  $C_l$ . This aspect shows that UVM is capable of revealing significant differences in prices, which should be taken into account by risk managers when selling policies. The use of an uncertain volatility model is able to point out discrepancies in prices that would otherwise go undetected.

## 7.2 Investigating the impact of stochastic interest rate on EIAs price

In this sub Section, we examine the impact of a stochastic interest rate model on the valuation of exchange-traded income annuities under the assumption of constant volatility. Given that the fund exhibits constant volatility, we employ the Black-Scholes Hull-White (BS HW) model. As in the previous sub Section, our study reviews the work developed by Cui et al. in [6], with a particular focus on Figure 5 of that paper. The parameters of the algorithm are given in Table 2, while the resulting graphs are presented in Figure 7.2. Specifically, we examine two yield curves published by the European Central Bank<sup>1</sup> for the euro area: one from September 2, 2020, representing a low-interest-rate environment, and another from September 2, 2024, reflecting high-interest-rate conditions. The resulting graphs share both similarities and differences with those presented by Cui et al.. Notably, we observe that prices increase with rising  $C_l$ . In the left graph, contrary to findings in [6], prices also increase with longer maturities. A similar trend is observed in the right graph, provided that  $C_l$  is not excessively low.

<sup>1</sup>For further details, see [https://www.ecb.europa.eu/stats/financial\\_markets\\_and\\_interest\\_rates/euro\\_area\\_yield\\_curves/html/index.en.html](https://www.ecb.europa.eu/stats/financial_markets_and_interest_rates/euro_area_yield_curves/html/index.en.html).

Model parameters			Product parameters		
Symbol	Meaning	Value	Symbol	Meaning	Value
$S_0$	Initial value of $S$	100	$T$	Maturity	1
$\sigma$	Volatility for BS case	variable	$M$	Number of monitoring dates	12
$\sigma_{\min}$	Lower bound for $\sigma$	$\sigma - 0.05$	$K$	Notional value	1
$\sigma_{\max}$	Upper bound for $\sigma$	$\sigma + 0.05$	$H$	Net/gross return switch	0
$\kappa$	Mean rev. speed of i.r.	1	$\gamma$	MCV factor	1
$\omega$	Volatility of i.r.	0	$F_l$	Local floor return	0
$\rho$	Correlation	0	$F_g$	Global floor return	0
$\eta$	Dividend yield	0	$C_l$	Local cap return	variable
			$C_g$	Global cap return	$9C_l$
			$\xi$	Surrender penalty	0
			$g$	guaranteed minimum rate	3%
			E. s.	Early surrender	No

Yield curve parameters			Algorithm parameters		
Symbol	Meaning	Value	Symbol	Meaning	Value
$\beta_0$	Long-term level	0.05	$N_L$	N. of time steps per period	256
$\beta_1$	Short-term slope	0	$N_S$	N. of grid refinements for $S$	16
$\beta_2$	Medium-term curvature	0	$N_Z$	N. of space points for $Z$	16
$\beta_3$	Long-term curvature	0	$N_\sigma$	N. of values for $\sigma$ optimization	100
$\tau_1$	Short-term decay factor	1			
$\tau_2$	Long-term decay factor	1			

Table 1: Parameters employed for numerical test in Sub Section 7.1.

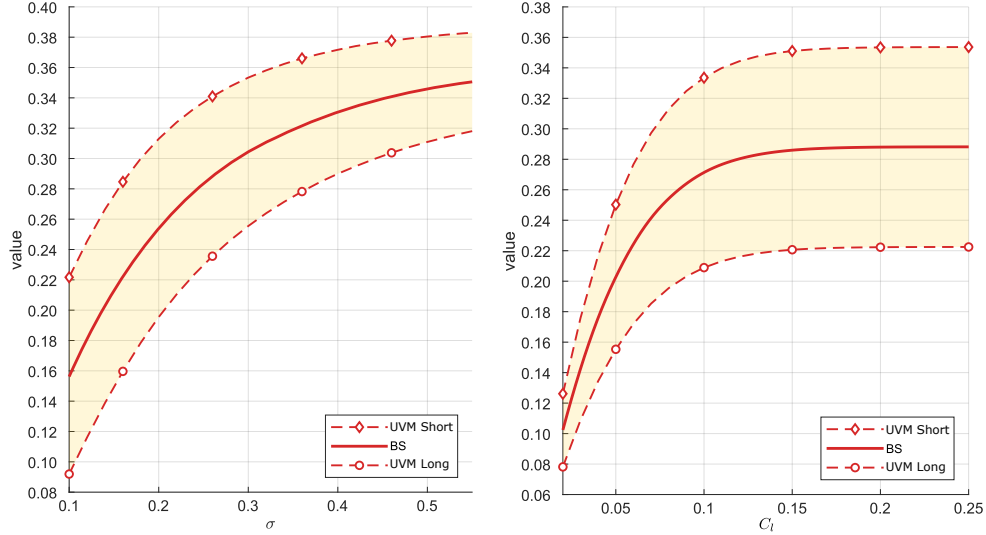


Figure 7.1: Comparison of EIAs prices under BS model and UVM with constant interest rate. (Left) BS model as  $\sigma$  varies and UVM model with volatility in  $[\sigma - 0.05, \sigma + 0.05]$  for  $C_l = 0.08$ . (Right) BS model with  $\sigma = 0.2$  and UVM model with volatility in  $[0.15, 0.25]$ .

Model parameters		Product parameters				Algorithm parameters		Yield curve parameters		
$S_0$	100	$T$	variable	$F_l$	0	$N_\tau$	256	Day	Sep. 2, 2020	Sep.2, 2024
$\sigma$	0.20	$M$	12	$F_g$	0	$N_S$	16	$\beta_0$	0.269446	0.503770
$\sigma_{\min}$	0.20	$K$	1	$C_l$	variable	$N_Z$	16	$\beta_1$	− 0.862654	3.051550
$\sigma_{\max}$	0.20	$H$	0	$C_g$	$10.8C_l$	$N_\sigma$	1	$\beta_2$	12.121820	− 1.578007
$\kappa$	0.2	$\gamma$	1	E.s.	No			$\beta_3$	−14.133376	6.467092
$\omega$	0.03							$\tau_1$	1.955330	1.710328
$\rho$	−0.3							$\tau_2$	2.105346	12.217401
$\eta$	0									

Table 2: Parameters employed for numerical test in Sub Section 7.2. See Table 1 for a summary explanation of the symbols listed here.

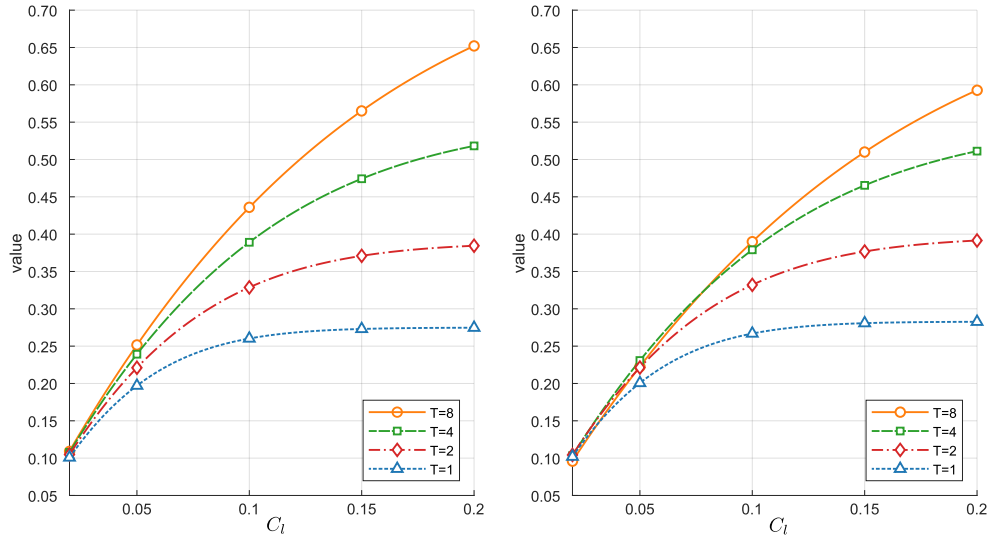


Figure 7.2: Comparison of EIAs prices under BS HW model, under the yield curve of September 2, 2020 (left) or September 2, 2024 (right).

### 7.3 Pricing EIAs in the UVM with stochastic interest rate without surrender risk

In this sub Section, we analyze the complete UVM Hull-White model and apply the Tree UVHW pricing algorithm to evaluate EIA contracts. We compare our results with those from the milestone paper [19] by Kijima and Wong, where the contract is assessed using a stochastic interest rate model. The contract parameters are provided in Table 3. It is worth noting that, for this contract, the returns are calculated on an annual basis.

First, we numerically investigate the convergence of the proposed method by varying both the number of discretization steps in the algorithm and the correlation coefficient  $\rho$ . Furthermore, we compute both the minimum and maximum prices under uncertain volatility, together with the price under certain volatility as determined by the BS HW model. The prices obtained using the Tree UVHW algorithm are reported in Table 4 for  $C_l = 16\%$  and in Table 5 for  $C = 20\%$ . To assess the quality of the results, we compare the obtained values with those calculated using two benchmark procedures. The first benchmark is GTU with  $M = 8000$  random-points and  $N_L = 64$  time steps per period; the second is a classic Monte Carlo with  $N_M = 10^7$  simulations, available only in the certain volatility model. In this latter case, the 95% confidence interval indicates an uncertainty of less than one hundredth for all the results reported in the Tables.

The results are very positive. In all the considered cases, the prices returned by the Tree UVHW are very similar to those of the benchmarks, and moreover, only a few seconds of computation are sufficient to obtain highly satisfactory results. On the other hand, please note that the benchmark computed with GTU requires approximately 8 hours of processing time. Conversely, the Monte Carlo method is very fast: only a few minutes are needed to obtain results accurate to the hundredth; however, this method is not applicable in the case of uncertain volatility. In conclusion, we can state that the proposed method converges quickly and that the computational time is reasonable, being much lower than that of GTU. Based on the numerical results just discussed, the algorithm configuration with  $N_L = 64$ ,  $N_S = 4$ ,  $N_Z = 4$ , and  $N_\sigma = 2$  returns very accurate results with a reasonable computation time. We will therefore use it as standard in subsequent tests, unless specified otherwise.

Now that these prices can be considered correct, let us briefly discuss the results qualitatively. It can be observed that the price recorded in the BS HW model invariably lies between the minimum (long) and maximum (short) prices, as expected. The difference between these two extreme prices are estimated at 12% and 13%, respectively, for  $C = 16\%$  and  $C = 20\%$ . Conversely, the impact of the correlation coefficient appears negligible, with a maximum price change of less than 1% observed across all cases when the coefficient varies from  $\rho = -0.3$  to  $\rho = 0.3$ .

Model parameters		Product parameters				Algorithm parameters		Yield curve parameters	
$S_0$	100	$T$	7	$F_l$	0	$N_L$	variable	Day	Sep.2, 2024
$\sigma$	0.25	$M$	7	$F_g$	$-\infty$	$N_S$	variable	$\beta_0$	0.503770
$\sigma_{\min}$	0.20	$K$	1	$C_l$	16% or 20%	$N_Z$	variable	$\beta_1$	3.051550
$\sigma_{\max}$	0.30	$H$	1	$C_g$	$+\infty$	$N_\sigma$	variable	$\beta_2$	− 1.578007
$\kappa$	0.2	$\gamma$	0.9	E.s.	variable			$\beta_3$	6.467092
$\omega$	0.03	$\xi$	0	$g$	3%			$\tau_1$	1.710328
$\rho$	−0.3, 0, +0.3							$\tau_2$	12.217401
$\eta$	0								

Table 3: Parameters employed for numerical test in Sub Section 7.3. See Table 1 for a summary explanation of the symbols listed here.

		Min price (Long)			BS HW price			Max price (Short)		
$\rho$		−0.3	0	0.3	−0.3	0	0.3	−0.3	0	0.3
Tree method with $N_S = 4, N_Z = 4, N_\sigma = 2$										
$N_L$	16	1.147 (1)	1.140 (1)	1.140 (1)	1.211 (1)	1.205 (1)	1.201 (1)	1.277 (1)	1.274 (1)	1.266 (1)
	32	1.145 (5)	1.140 (5)	1.138 (5)	1.210 (3)	1.205 (3)	1.200 (3)	1.278 (5)	1.273 (5)	1.266 (5)
	64	1.144 (28)	1.140 (30)	1.137 (28)	1.210 (18)	1.205 (17)	1.200 (17)	1.278 (29)	1.273 (30)	1.267 (29)
	128	1.144 (189)	1.139 (190)	1.137 (204)	1.210 (284)	1.205 (310)	1.200 (236)	1.278 (313)	1.273 (498)	1.267 (461)
Tree method with $N_S = 8, N_Z = 8, N_\sigma = 8$										
$N_L$	16	1.146 (24)	1.141 (7)	1.140 (23)	1.211 (3)	1.205 (2)	1.201 (2)	1.278 (19)	1.274 (7)	1.266 (21)
	32	1.145 (128)	1.141 (34)	1.138 (122)	1.210 (25)	1.205 (26)	1.201 (25)	1.278 (149)	1.273 (33)	1.267 (74)
	64	1.144 (459)	1.140 (105)	1.137 (405)	1.210 (65)	1.205 (65)	1.200 (66)	1.279 (404)	1.273 (104)	1.267 (403)
	128	1.143 (3532)	1.139 (785)	1.136 (3158)	1.210 (488)	1.205 (492)	1.200 (657)	1.279 (4310)	1.273 (2094)	1.268 (4157)
Benchmarks										
MC					1.209	1.205	1.200			
GTU		1.144	1.140	1.137	1.210	1.206	1.201	1.280	1.274	1.268

Table 4: Convergence of the Tree UVHW method with local cap  $C_l = 16\%$ . Early surrender is not allowed. The values in parentheses represent the computational times, measured in seconds.

		Min price (Long)			BS-HW price			Max price (Short)		
$\rho$		-0.3	0	0.3	-0.3	0	0.3	-0.3	0	0.3
Tree method with $N_S = 4, N_Z = 4, N_\sigma = 2$										
$N_L$	16	1.194 (1)	1.189 (1)	1.186 (1)	1.269 (1)	1.261 (1)	1.258 (1)	1.347 (1)	1.340 (1)	1.334 (1)
	32	1.193 (5)	1.187 (5)	1.185 (5)	1.269 (3)	1.263 (3)	1.258 (3)	1.347 (5)	1.342 (5)	1.334 (5)
	64	1.192 (29)	1.187 (29)	1.184 (30)	1.268 (18)	1.263 (18)	1.257 (18)	1.347 (30)	1.342 (30)	1.335 (30)
	128	1.191 (197)	1.186 (210)	1.183 (344)	1.268 (128)	1.263 (129)	1.257 (129)	1.348 (218)	1.342 (219)	1.335 (214)
Tree method with $N_S = 8, N_Z = 8, N_\sigma = 8$										
$N_L$	16	1.194 (10)	1.190 (3)	1.187 (10)	1.270 (2)	1.261 (2)	1.259 (2)	1.347 (11)	1.341 (3)	1.334 (11)
	32	1.192 (64)	1.187 (18)	1.185 (64)	1.269 (11)	1.263 (11)	1.258 (11)	1.347 (63)	1.342 (17)	1.335 (66)
	64	1.191 (422)	1.187 (108)	1.183 (425)	1.268 (68)	1.263 (68)	1.258 (68)	1.348 (419)	1.342 (111)	1.335 (420)
	128	1.191 (3175)	1.186 (792)	1.183 (3010)	1.268 (490)	1.263 (500)	1.257 (498)	1.348 (3030)	1.342 (798)	1.335 (3038)
Benchmarks										
MC					1.268	1.262	1.257			
GTU		1.192	1.188	1.184	1.269	1.264	1.258	1.349	1.342	1.336

Table 5: Convergence of the Tree UVHW method with local cap  $C_l = 20\%$ . Early surrender is not allowed. The values in parentheses represent the computational times, measured in seconds.

## 7.4 Pricing EIAs in the UVM with stochastic interest rate with surrender risk

We proceed by investigating the convergence of the Tree UVHW in scenarios where early surrender is a possibility. The outcomes of this analysis are presented in Tables 6 and 7, respectively, for  $C_l = 16\%$  and  $C_l = 20\%$ . A comparative analysis is then conducted with the results obtained from GTU and Monte Carlo methods (this latter only in the case of constant volatility), utilizing an optimization approach based on the Longstaff-Schwartz method. The prices returned by the Tree UVHW are found to be in close agreement with those obtained from the benchmark methods, and good approximations of the limiting values can be achieved within a matter of seconds. For the sake of completeness, it should be noted that the computational times required to compute the benchmark prices are very high, amounting to several hours for both GTU and Monte Carlo.

Beyond numerical considerations, it is interesting to observe that the final price is significantly affected by the chosen strategy: moving from the long strategy to the short strategy increases the price by approximately 10% for  $C_l = 16\%$  and 12% for  $C_l = 20\%$ . Moreover, we can observe that the short strategy invariably returns a higher price than the mixed strategy, as anticipated, though the disparity is marginal, amounting to less than 1% for both values of  $C_l$ . Moreover, in a manner similar to the context of prohibited early surrender, the influence of the correlation coefficient  $\rho$  appears to be negligible. Finally, it should be noted that, as is natural, all prices obtained by allowing early surrender are higher than the respective prices without such an option, reported in Tables 4 and 5. In particular, the increase varies between 1% and 2%. This also applies when comparing the mixed strategy with the short strategy without early exercise.

We conclude this sub Section by analyzing the optimal operating region for a contract with  $C_l = 16\%$  and  $\rho = -0.3$ . In particular, we study the qualitative properties that emerge when comparing the optimal exercise strategies under both long and short positions. It is interesting to note that, given the parameters in Table 1, the exercise value at monitoring date  $m$  for this contract is given by

$$\Psi(X_m, G_m) = \max(1 + Z_m, (1 + g)^m).$$

Therefore, the optimal strategy is to exercise the option at the first contract anniversary  $m$  such that the continuation value  $\mathcal{C}_m(Z_m, R_m)$  is less than  $1 + Z_m$ ,  $(1 + g)^m$ , or both. For this reason, in the graphs shown in Figure 7.3, three cases are highlighted: in the red region the inequality  $(1 + g)^m \geq \mathcal{C}_m(Z_m, R_m) > 1 + Z_m$  is satisfied, in the blue region  $1 + Z_m \geq \mathcal{C}_m(Z_m, R_m) > (1 + g)^m$  and in the green region both inequalities  $(1 + g)^m \geq \mathcal{C}_m(Z_m, R_m)$  and  $1 + Z_m \geq \mathcal{C}_m(Z_m, R_m)$  are satisfied. Finally, the white region corresponds to points where early exercise is not convenient, that is  $\mathcal{C}_m(Z_m, R_m) > \Psi(X_m, G_m)$ . In particular, these graphs illustrate the optimal choices as a function of the value of  $Z_m \in [0, mC_l]$  and the interest rate  $r_m \in [-2\%, 12\%]$  (used in place of  $R_m$  to facilitate the economic interpretation of the results). We also distinguish the optimal strategy for a long position (left) from that for a short position (right).

In general, it can be stated that, for all cases considered, it is advantageous to terminate the contract early when the interest rate  $r$  is high. The reason for this phenomenon lies in the local cap on growth,  $C_l$ , which limits the contract's value appreciation despite high growth rates of the underlying equity index under risk-neutral probability. This effect is more pronounced in the case of a short position: the policyholder, fearing a loss in the contract's value, prefers to exit early, favoring certainty over uncertainty.

The dependence on  $Z_m$  is less evident: as  $Z_m$  increases, both the continuation value and the linear factor  $1 + Z_m$  grow, while the constant term  $(1 + g)^m$  remains unaffected by  $Z_m$ . Moreover, the growth of the



		Min price (Long)			BS HW price			Mixed strategy			Max price (Short)		
$\rho$		-0.3	0	0.3	-0.3	0	0.3	-0.3	0	0.3	-0.3	0	0.3
Tree method with $N_S = 4, N_Z = 4, N_\sigma = 2$													
$N_L$	16	1.172 (1)	1.169 (1)	1.172 (1)	1.229 (1)	1.226 (1)	1.226 (1)	1.283 (2)	1.282 (2)	1.277 (2)	1.291 (1)	1.290 (1)	1.285 (1)
	32	1.170 (5)	1.169 (5)	1.170 (5)	1.228 (3)	1.226 (3)	1.225 (3)	1.283 (10)	1.281 (10)	1.277 (10)	1.291 (5)	1.289 (5)	1.285 (5)
	64	1.169 (30)	1.169 (30)	1.169 (30)	1.228 (18)	1.226 (18)	1.225 (18)	1.284 (60)	1.281 (60)	1.278 (60)	1.292 (31)	1.289 (31)	1.286 (31)
	128	1.169 (199)	1.168 (198)	1.169 (197)	1.228 (119)	1.226 (119)	1.225 (115)	1.284 (392)	1.281 (389)	1.278 (387)	1.292 (196)	1.289 (197)	1.286 (198)
Tree method with $N_S = 8, N_Z = 8, N_\sigma = 8$													
$N_L$	16	1.172 (10)	1.170 (3)	1.172 (9)	1.229 (2)	1.226 (2)	1.226 (2)	1.283 (19)	1.282 (6)	1.277 (19)	1.291 (10)	1.290 (3)	1.285 (10)
	32	1.170 (56)	1.169 (16)	1.170 (60)	1.229 (10)	1.226 (10)	1.225 (10)	1.283 (114)	1.281 (31)	1.278 (115)	1.292 (58)	1.289 (16)	1.286 (55)
	64	1.169 (375)	1.169 (100)	1.169 (379)	1.228 (59)	1.226 (60)	1.225 (61)	1.284 (745)	1.281 (197)	1.278 (747)	1.292 (381)	1.289 (100)	1.286 (377)
	128	1.169 (3056)	1.168 (803)	1.169 (3054)	1.228 (498)	1.226 (503)	1.225 (501)	1.284 (6282)	1.281 (1592)	1.278 (7520)	1.292 (3153)	1.289 (802)	1.286 (3060)
Benchmarks													
MC					1.227	1.225	1.223						
GTU		1.169	1.169	1.169	1.229	1.227	1.226	1.285	1.282	1.279	1.293	1.290	1.287

Table 6: Convergence of the Tree UVHW method with local cap  $C_l = 16\%$ . Early surrender is allowed at monitoring dates. The values in parentheses represent the computational times, measured in seconds.

		Min price (Long)			BS HW price			Mixed strategy			Max price (Short)		
$\rho$		-0.3	0	0.3	-0.3	0	0.3	-0.3	0	0.3	-0.3	0	0.3
Tree method with $N_S = 4, N_Z = 4, N_\sigma = 2$													
$N_L$	16	1.213 (1)	1.211 (1)	1.212 (1)	1.282 (1)	1.277 (1)	1.278 (1)	1.348 (2)	1.344 (2)	1.341 (3)	1.356 (1)	1.352 (1)	1.349 (1)
	32	1.211 (5)	1.209 (5)	1.210 (5)	1.282 (3)	1.279 (3)	1.277 (3)	1.348 (10)	1.346 (9)	1.341 (10)	1.357 (5)	1.354 (5)	1.349 (5)
	64	1.210 (30)	1.209 (30)	1.209 (30)	1.281 (18)	1.279 (18)	1.277 (18)	1.349 (59)	1.345 (59)	1.341 (60)	1.357 (31)	1.354 (31)	1.349 (30)
	128	1.210 (205)	1.209 (203)	1.209 (199)	1.281 (118)	1.279 (117)	1.277 (120)	1.349 (389)	1.345 (387)	1.341 (391)	1.357 (194)	1.354 (197)	1.350 (198)
Tree method with $N_S = 8, N_Z = 8, N_\sigma = 8$													
$N_L$	16	1.213 (9)	1.212 (3)	1.212 (9)	1.283 (2)	1.277 (2)	1.278 (2)	1.349 (20)	1.345 (6)	1.341 (20)	1.357 (10)	1.353 (3)	1.349 (10)
	32	1.211 (66)	1.209 (17)	1.210 (64)	1.282 (11)	1.280 (11)	1.277 (10)	1.348 (114)	1.346 (31)	1.341 (116)	1.357 (59)	1.354 (17)	1.349 (60)
	64	1.210 (379)	1.209 (99)	1.209 (382)	1.281 (61)	1.279 (59)	1.277 (58)	1.349 (772)	1.345 (200)	1.341 (1032)	1.357 (423)	1.354 (108)	1.350 (416)
	128	1.210 (3004)	1.209 (796)	1.209 (3042)	1.281 (494)	1.279 (501)	1.277 (494)	1.348 (6054)	1.345 (1585)	1.341 (6067)	1.357 (3037)	1.354 (798)	1.350 (3035)
Benchmarks													
MC					1.281	1.278	1.276						
GTU		1.210	1.210	1.209	1.282	1.280	1.278	1.350	1.346	1.342	1.358	1.354	1.351

Table 7: Convergence of the Tree UVHW method with local cap  $C_l = 20\%$ . Early surrender is allowed at monitoring dates. The values in parentheses represent the computational times, measured in seconds.

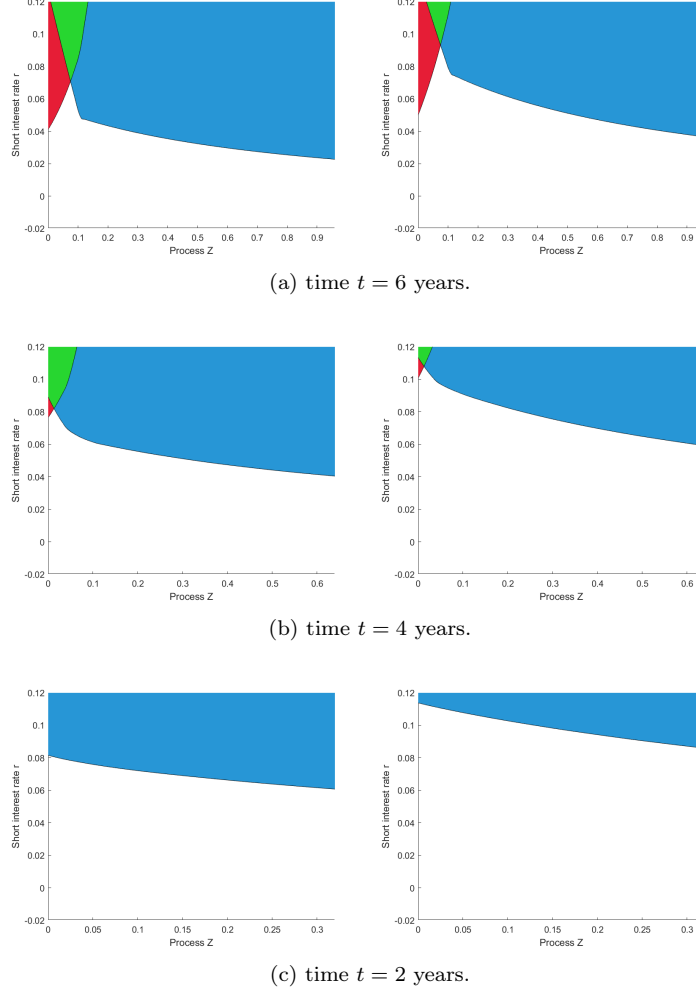


Figure 7.3: Optimal surrender region for long (left) and short (right) position for different monitoring dates. The colored region denotes where early exercise is convenient.

continuation value is sublinear because the payoff is capped due to the cap on  $Z_m$ . Consequently, for high values of  $Z_m$ , early exercise is advantageous due to the  $1 + Z_m$  factor (observe the blue region), while, for low values of  $Z_m$ , it is beneficial due to the  $(1 + g)^m$  factor (observe the red region). For intermediate values of  $Z_m$ , early exercise may be advantageous due to both factors (observe the green region) or disadvantageous (observe the white region), depending on the specific circumstances.

Finally, it is important to note that the convenience of early exercise is limited in the initial years, while it becomes more feasible as time progresses. This is due to the fact that by engaging in exercise at an early stage, an individual relinquishes the future benefits provided by the floor in all subsequent monitoring dates.

## 8 Conclusion

In this paper, we have developed a novel tree-based numerical method for pricing equity-indexed annuities, featuring cliquet-style guarantees and early surrender risk. Our model integrates an uncertain volatility framework for the underlying asset with a stochastic interest rate modeled by the Hull-White dynamics, thereby providing a robust approach for addressing market uncertainties. This aspect highlights that UVM enables robust pricing by uncovering significant price differences, which risk managers should consider when selling policies. Additionally, we have shown that it is important to consider a stochastic interest rate model capable of accurately capturing rate dynamics, which play a crucial role in these long-maturity insurance products. The proposed Tree UVHW algorithm has been extensively tested and demonstrates high accuracy and computational efficiency when compared to benchmark methods such as Monte Carlo simulations and the GTU algorithm. Our numerical experiments confirm that both volatility uncertainty and the stochastic behavior of interest rates play a significant role in determining the value of these complex financial products. In particular, the inclusion of an early surrender option leads to differentiated optimal exercise strategies, with distinct implications for short and long positions. Overall, our findings underscore the importance of employing flexible modeling frameworks and efficient numerical techniques in the valuation of exotic, path-dependent contracts.

## A Appendix: proof of Proposition 1

Ostrovski [21] has already demonstrated that the random variables  $(R_{t+\Delta t} - R_t \mid R_t)$  and  $(I_{t+\Delta t} - I_t \mid R_t)$  follow a Gaussian distribution, as well as established their associated mean, variance, and covariance indicators. In addition, by definition,  $W_{t+\Delta t}^S - W_t^S$  follows a Gaussian distribution, with zero mean and variance equal to  $\Delta t$ , which is independent by  $R_t$ , so it has the same law of  $(W_{t+\Delta t}^S - W_t^S \mid R_t)$ . Only the covariance formulas between  $(W_{t+\Delta t}^S - W_t^S \mid R_t)$  and the other two random variables remain to be proved. We start by computing the correlations between the increment  $(W_{t+\Delta t}^r - W_t^r \mid R_t)$  and the other two random variables.

The process  $R$  follows the Vasicek model, and standard calculations for this type of process (see e.g. Brigo and Mercurio [3]) allow solving the associated SDE, yielding:

$$R_{t+\Delta t} = e^{-\kappa\Delta t} \left( R_t + \int_t^{t+\Delta t} e^{\kappa(s-t)} dW_s^r \right).$$

Therefore, we can write

$$\begin{aligned} \text{Cov} \left[ (R_{t+\Delta t} - R_t \mid R_t), (W_{t+\Delta t}^r - W_t^r \mid R_t) \right] &= \text{Cov} \left[ e^{-\kappa\Delta t} \int_t^{t+\Delta t} e^{\kappa(s-t)} dW_s^r, \int_t^{t+\Delta t} dW_s^r \right] \\ &= e^{-\kappa\Delta t} \text{Cov} \left[ \int_t^{t+\Delta t} e^{\kappa(s-t)} dW_s^r, \int_t^{t+\Delta t} dW_s^r \right] \\ &= e^{-\kappa\Delta t} \int_t^{t+\Delta t} e^{\kappa(s-t)} ds \\ &= \frac{1 - e^{-\kappa\Delta t}}{\kappa}. \end{aligned}$$

$$\begin{aligned}
\mathbb{Cov} \left[ (I_{t+\Delta t} - I_t \mid R_t), (W_{t+\Delta t}^r - W_t^r \mid R_t) \right] &= \mathbb{Cov} \left[ \int_t^{t+\Delta t} R_s ds, \int_t^{t+\Delta t} dW_s^r \right] \\
&= \mathbb{Cov} \left[ \int_t^{t+\Delta t} e^{-\kappa(s-t)} \left( R_t + \int_t^s e^{\kappa(u-t)} dW_u^r \right) ds, \int_t^{t+\Delta t} dW_s^r \right] \\
&= \mathbb{Cov} \left[ \int_t^{t+\Delta t} \int_t^s e^{-\kappa(s-u)} dW_u^r ds, \int_t^{t+\Delta t} dW_s^r \right] \\
&= \mathbb{Cov} \left[ \int_t^{t+\Delta t} \int_u^{t+\Delta t} e^{-\kappa(s-u)} ds dW_u^r, \int_t^{t+\Delta t} dW_s^r \right] \\
&= \mathbb{Cov} \left[ \frac{1}{\kappa} \int_t^{t+\Delta t} 1 - e^{-\kappa(t+\Delta t-u)} dW_u^r, \int_t^{t+\Delta t} dW_s^r \right] \\
&= \frac{1}{\kappa} \int_t^{t+\Delta t} 1 - e^{-\kappa(t+\Delta t-u)} du \\
&= \frac{1}{\kappa^2} (\kappa \Delta t + e^{-\kappa \Delta t} - 1)
\end{aligned}$$

We emphasize that the interchange of the two integrals, which occurs in the fourth line of the previous calculation, is justified by the Fubini-Tonelli Theorem. Specifically, this theorem allows the reversal of the order of integration in double integrals under certain conditions. In this case, the function  $e^{-\kappa(s-u)}$  is continuous and integrable over the region of integration, which is the triangular domain defined by  $t \leq u \leq s \leq t + \Delta t$ . This region is measurable, and the integrand is non-negative and bounded. Therefore, we can safely exchange the order of integration without violating any conditions for the application of Fubini's Theorem. This leads to the simplified expression for the covariance calculation.

Now, we come back to the Gaussian increment  $W_{t+\Delta t}^S - W_t^S$ . Since  $W^S$  and  $W^r$  are correlated, we can write

$$W_{t+\Delta t}^S - W_t^S = \rho (W_{t+\Delta t}^r - W_t^r) + \sqrt{1 - \rho^2} G$$

with  $G \sim \mathcal{N}(0, \Delta t)$  a Gaussian random variable independent from all the other random variables. Then

$$\begin{aligned}
\mathbb{Cov} \left[ (R_{t+\Delta t} - R_t \mid R_t), (W_{t+\Delta t}^r - W_t^r \mid R_t) \right] &= \mathbb{Cov} \left[ R_{t+\Delta t} - R_t \mid R_t, \rho (W_{t+\Delta t}^r - W_t^r) + \sqrt{1 - \rho^2} G \mid R_t \right] \\
&= \mathbb{Cov} \left[ R_{t+\Delta t} - R_t \mid R_t, \rho (W_{t+\Delta t}^r - W_t^r) \mid R_t \right] \\
&= \frac{\rho}{\kappa} (1 - e^{-\kappa \Delta t}).
\end{aligned}$$

$$\begin{aligned}
\mathbb{Cov} \left[ (I_{t+\Delta t} - I_t \mid R_t), (W_{t+\Delta t}^r - W_t^r \mid R_t) \right] &= \mathbb{Cov} \left[ I_{t+\Delta t} - I_t \mid R_t, \rho (W_{t+\Delta t}^r - W_t^r) + \sqrt{1 - \rho^2} G \mid R_t \right] \\
&= \frac{\rho}{\kappa^2} (\kappa \Delta t + e^{-\kappa \Delta t} - 1).
\end{aligned}$$

## B Appendix: proof of Proposition 2

According to Proposition 1, we can write

$$\left( \begin{array}{c} R_{t+\Delta t} - R_t \\ W_{t+\Delta t}^S - W_t^S \end{array} \right) \mid R_t \sim \mathcal{N} \left( \left( \begin{array}{c} \mu_R \\ \mu_W \end{array} \right), \left( \begin{array}{cc} \sigma_R^2 & \sigma_{R,W} \\ \sigma_{R,W} & \sigma_W^2 \end{array} \right) \right),$$

with

$$\mu_R = R_t (e^{-\kappa\Delta t} - 1), \mu_W = 0, \sigma_R^2 = \frac{1}{2\kappa} (1 - e^{-2\kappa\Delta t}), \sigma_W^2 = \Delta t, \text{ and } \sigma_{R,W} = \frac{\rho}{\kappa} (1 - e^{-\kappa\Delta t}).$$

Now, let us define the linear coefficient of correlation between  $R_{t+\Delta t} - R_t \mid R_t$  and  $W_{t+\Delta t}^S - W_t^S \mid R_t$  as

$$\rho_{W,R} = \frac{\sigma_{R,W}}{\sqrt{\sigma_R^2 \sigma_W^2}}.$$

A standard result about conditional Gaussian distributions (see e.g. Theorem 3.5 in DasGupta [7]) allows us to compute the distribution of the Gaussian increment  $W_{t+\Delta t}^S - W_t^S$  given the values  $R_t$  and  $R_{t+\Delta t}$  as follows:

$$(W_{t+\Delta t}^S - W_t^S \mid R_{t+\Delta t}, R_t) \sim \mathcal{N}(\mu_{W|R}, \sigma_{W|R}^2),$$

with

$$\begin{aligned} \mu_{W|R} &= \mu_W + \rho_{W,R} \sqrt{\frac{\sigma_W^2}{\sigma_R^2}} (R_{t+\Delta t} - \mu_R) \\ &= \mu_W + \frac{\sigma_{R,W}}{\sigma_R^2} (R_{t+\Delta t} - \mu_R) \\ &= 0 + \frac{\rho \frac{1-e^{-\kappa\Delta t}}{\kappa}}{\frac{1}{2\kappa} (1 - e^{-2\kappa\Delta t})} (R_{t+\Delta t} - R_t e^{-\kappa\Delta t}) \\ &= 2\rho \frac{1 - e^{-\kappa\Delta t}}{1 - e^{-2\kappa\Delta t}} (R_{t+\Delta t} - R_t e^{-\kappa\Delta t}), \end{aligned}$$

and

$$\begin{aligned} \sigma_{W|R}^2 &= \sigma_W^2 (1 - \rho_{W,R}^2) \\ &= \sigma_W^2 - \frac{(\sigma_{R,W})^2}{\sigma_R^2} \\ &= \Delta t - \frac{\left(\rho \frac{1-e^{-\kappa\Delta t}}{\kappa}\right)^2}{\frac{1}{2\kappa} (1 - e^{-2\kappa\Delta t})} \\ &= \Delta t - 2 \frac{\rho^2}{\kappa} \frac{1 - e^{-\kappa\Delta t}}{1 + e^{-\kappa\Delta t}}. \end{aligned}$$

## Acknowledgement

This work was supported by the Departmental Strategic Plan (PSD) of the University of Udine, *Interdepartmental Project on Artificial Intelligence (2020-2025)*.

## Disclosure statement

No potential conflict of interest was reported by the authors.

## References

- [1] Marco Avellaneda, Arnon Levy, and Antonio Parás. Pricing and hedging derivative securities in markets with uncertain volatilities. *Applied Mathematical Finance*, 2(2):73–88, 1995.

- [2] Maya Briani, Lucia Caramellino, and Antonino Zanette. A hybrid approach for the implementation of the Heston model. *IMA Journal of Management Mathematics*, 28(4):467–500, 2017.
- [3] Damiano Brigo and Fabio Mercurio. *Interest Rate Models: Theory and Practice*, volume 2. Springer, 2001.
- [4] Massimo Costabile, Ivar Massabó, and Emilio Russo. Evaluating variable annuities with GMWB when exogenous factors influence the policy-holder’s withdrawals. *The European Journal of Finance*, 26(2-3):238–257, 2020.
- [5] John C. Cox, Stephen A. Ross, and Mark Rubinstein. Option pricing: A simplified approach. *Journal of Financial Economics*, 7(3):229–263, 1979.
- [6] Zhenyu Cui, J Lars Kirkby, and Duy Nguyen. Equity-linked annuity pricing with cliquet-style guarantees in regime-switching and stochastic volatility models with jumps. *Insurance: Mathematics and Economics*, 74:46–62, 2017.
- [7] Anirban DasGupta. *Probability for Statistics and Machine Learning: Fundamentals and Advanced Topics*. Springer, New York, NY, 2011.
- [8] Hans U Gerber and Elias SW Shiu. Pricing lookback options and dynamic guarantees. *North American Actuarial Journal*, 7(1):48–66, 2003.
- [9] Ludovic Goudenège, Andrea Molent, and Antonino Zanette. Pricing and hedging GLWB in the Heston and in the Black–Scholes with stochastic interest rate models. *Insurance: Mathematics and Economics*, 70:38–57, 2016.
- [10] Ludovic Goudenège, Andrea Molent, and Antonino Zanette. Leveraging machine learning for high-dimensional option pricing within the Uncertain Volatility Model. *arXiv preprint arXiv:2407.13213*, 2024.
- [11] P. A. Forsyth H. A. Windcliff and K. R. Vetzal. Numerical methods and volatility models for valuing cliquet options. *Applied Mathematical Finance*, 13(4):353–386, 2006.
- [12] Mary Hardy. Investment guarantees; modeling and risk management for equity linked life insurance. *John Wiley & Sons*, 2003.
- [13] Patrick Hénaff and Claude Martini. Model validation: theory, practice and perspectives. *Zeliade White Paper*, 2010.
- [14] Markus Hess. Cliquet option pricing in a jump-diffusion Lévy model. *Modern Stochastics: Theory and Applications*, 5(3):317–336, 2018.
- [15] Peter Hieber. Cliquet-style return guarantees in a regime switching Lévy model. *Insurance: Mathematics and Economics*, 72:138–147, 2017.
- [16] Julian Hölzermann. The Hull–White model under volatility uncertainty. *Quantitative Finance*, 21(11):1921–1933, 2021.
- [17] Julian Hölzermann. Pricing interest rate derivatives under volatility uncertainty. *Annals of Operations Research*, 336(1):153–182, 2024.

- [18] Robert A. Jarrow and Andrew Rudd. *Option Pricing*. Richard D. Irwin, Homewood, IL, 1983.
- [19] Masaaki Kijima and Tony Wong. Pricing of ratchet equity-indexed annuities under stochastic interest rates. *Insurance: Mathematics and Economics*, 41(3):317–338, 2007.
- [20] Daniel B Nelson and Krishna Ramaswamy. Simple binomial processes as diffusion approximations in financial models. *The Review of Financial Studies*, 3(3):393–430, 1990.
- [21] Vladimir Ostrovski. Efficient and exact simulation of the Hull-White model. *Available at SSRN 2304848*, 2013.
- [22] Williams C. K. I. Rasmussen, C. E. Gaussian Processes for Machine Learning, 2006.
- [23] X Sheldon Lin and Ken Seng Tan. Valuation of equity-indexed annuities under stochastic interest rates. *North American Actuarial Journal*, 7(4):72–91, 2003.
- [24] Adam T Smith. American options under uncertain volatility. *Applied Mathematical Finance*, 9(2):123–141, 2002.
- [25] Lars EO Svensson. Estimating and interpreting forward interest rates: Sweden 1992-1994, 1994.
- [26] Song Wang. Pricing european call options with interval-valued volatility and interest rate. *Applied Mathematics and Computation*, 474:128698, 2024.
- [27] Xiao Wei, Marcellino Gaudenzi, and Antonino Zanette. Pricing ratchet equity-indexed annuities with early surrender risk in a CIR++ model. *North American Actuarial Journal*, 17(3):229–252, 2013.
- [28] Paul Wilmott. Cliquet options and volatility models. *The best of Wilmott*, page 379, 2002.